A Survey of the Gas-Phase Negative Ion Kinetics of Inorganic Molecules. Electron Attachment Reactions

G. E. CALEDONIA*

Avco Everett Research Laboratory, Inc., a Subsidiary of Avco Corporation, Everett, Massachusetts

Received April 2, 1974 (Revised Manuscript Received June 27, 1974)

Contents

I. Introduction

In recent years a large amount of information on the reaction kinetics of negative ions has appeared in the literature. This research reflects the importance of negative ion kinetics in a diverse number of fields including upper atmospheric studies, reentry physics, gaseous electrical discharges, and laser physics. The author is presently engaged in developing a survey, with critical analysis, of the available theoretical analysis and experimental reaction rate data for gas-phase negative ion reactions of inorganic molecules. The survey will be limited to exothermic or slightly endothermic reactions, and the rate constant data considered will correspond to measurements made under conditions of thermal equilibrium, i.e., ion/electron temperature $\approx$ translational temperature, at temperatures typically less than 3000°K although in specific instances higher energy data may be cited. This report encompasses the first two sections of the survey, concerned with three-body and dissociative electron attachment.

The main emphasis of the survey is on the discussion of reactions between electrons, negative ions, and neutrals of importance in the $O_2/N_2/H_2O/CO_2$ system. All possible exothermic reactions of this system are considered and, where possible, undetermined rate constants are estimated. However, the survey is quite general and an attempt has been made to include all the rate constant data of negative ion reactions studied under conditions of thermal equilibrium. While these additional reactions are interesting in their own right, they also provide a larger data base for observing trends in particular types of negative ion reactions and may be of use in estimating rate constants. Reactions which have been explicitly excluded from the survey include those involving large molecules, i.e., SF_6, CCl_4, etc., and hydrocarbons. A limited number of references to the recent literature on such reactions will be included in the text.

The report is broken into sections by reaction type. Each section includes a detailed discussion along with the tabulated rate constant data. The reactions in each section are ordered with increasing reactant size (i.e., monatomic, diatomic, etc.), and alphabetically for a given reactant size. Rate constant entries for a given reaction are listed chronologically. In cases where rate constant measurements for a specific reaction are in conflict a recommended value will be followed by an asterisk. It should be pointed out that such recommendations may be based on the author's personal preference since there is frequently insufficient information available to determine a preferred rate constant in an objective manner.

Excellent discussions on the various experimental methods used in measuring the rate constants of negative ion reactions may be found in recent texts by McDaniel et al.[1] and Christophorou[2] among others. In the text the experimental technique by which a specific rate constant was determined is designated by a letter following the relevant reference number. The meaning of the letters is given in Table I. A separate letter is used to indicate those experiments where mass spectrometry was used to identify the reaction products. Symbols are also used to designate those rate constants which were determined indirectly, either by detailed balancing or extrapolation or by theoretical prediction. The types of experiments listed in Table I are quite general and there can, of course, be major differences in experimental technique between any two studies using similar apparatus. The exothermicity (or endothermicity) of each reaction is also tabulated along with the temperature and pressure (if relevant) at which the measurements were made.

Where required, the Langevin rate constant[3,4] is used as a measure of the maximum allowable rate constant for an ion–neutral reaction. This theoretical prediction is based on the assumption that the interaction potential may be described by the induced dipole field between the reactants. The resulting expression is[4]

$$k = 2\pi e(\alpha/\mu)^{1/2} \qquad (1)$$

where e is the electronic charge, μ is the reduced mass of the reactants, and α is the polarizability of the neutral reactant. While there has been some criticism[5] as to the general use of this formalism in describing ion–molecule kinetics, it appears to be most appropriate at thermal energies and is useful as a measure of the efficiency of a given reaction.

TABLE I. Code Description

Designation	Meaning	Designation	Meaning
a	Drift tube (Swarm)	f	Flame
b	Stationary afterglow	g	Mass analysis
c	Flowing afterglow	h	Theoretical prediction
d	Electron beam	i	Detailed balancing of reverse rate constant
e	Shock tube	j	Extrapolated from higher energy data

* Presently at Physical Sciences Inc., Wakefield, Mass. 01880.

II. Three-Body Attachment of Electrons to Atoms and Molecules

The available measurements and predictions for the rate of three-body attachment to atoms and molecules of interest in this survey are summarized in Table II. The general form of such reactions is

$$e + X + M \underset{k_d}{\overset{k_a}{\rightleftarrows}} X^- + M \qquad (2)$$

The discussion below is divided into sections according to the size of the attaching species.

A. Atoms

While some theoretical effort[6-8] has been directed to the prediction of the cross sections for three-body attachment of electrons to atoms, the results are generally not readily applicable to situations characterized by thermal equilibrium at relatively low temperatures. Perhaps the most directly applicable work is that of Shui and Keck[8] who have recently developed a modified phase space theory for the prediction of the collisional detachment (the reverse of reaction 2) rate constants of atomic negative ions. This theory requires a parameter which describes the interaction potential between the negative ion and its collision partner and as yet no a priori technique has been developed to predict this quantity. However, predictions of the theory, where the unknown parameter was chosen empirically, have been found to be in good agreement, in both magnitude and temperature dependence, with high temperature (>3000°K) data on collisional detachment of the halogen negative ions.[8]

The experimental data base for the attachment of electrons to atoms is relatively sparse. The most direct attempt to study such a reaction would appear to be the research of Good[9] on the attachment of electrons to fluorine atoms. In this study the attachment process was found to proceed with a rather remarkable positive activation energy of 3.6 eV. The experimental technique consisted of shock heating mixtures of air and fluorine containing species, such as SF_6 and CF_4, to temperatures of ≈3800°K and pressures of ~1.5 atm. Under these conditions the fluorine in the mixture was completely converted to atomic form. The shock heated gas was then expanded in a nozzle, and the resulting electron density history was monitored via microwave techniques.

In the clean air cases it was reported that the electron decay in the nozzle was due solely to the volume expansion, i.e.

$$dn_e/dt = n_e \, d \ln (N)/dt \qquad (3)$$

where n_e is the electron density in parts/cc and N is the total number density. The difference between the electron decay rate in pure air and that in fluorine contaminated mixtures was ascribed to attachment by F atoms, and the relevant attachment rate constant was determined by use of the relationship

$$d(n_e - n_{e_A})/dt = -k_a n_e F N \qquad (4)$$

where n_{e_A} is the electron density in clean air, n_e that in the fluorine contaminated mixture, F the F-atom concentration, N the total number density, and k_a the attachment rate. The activation energy was deduced by determining the variation of k_a along the nozzle. The rate constant was found to increase by a factor of 10 as the temperature was decreased from 2800 to 2400°K. This analysis was in error, however, since it can be readily shown that the governing equation actually is

$$d(n_e - n_{e_A})/dt = -k_a' n_e F N + (n_e - n_{e_A}) \, d \ln (N)/dt \qquad (5)$$

Comparing this with (4) one finds that the relation between the actual attachment rate, k_a', and the value of k_a deduced by Good is

$$k_a = k_a' + \frac{(n_{e_A}/n_e - 1)}{FN} d \ln (N)/dt \qquad (6)$$

The experiment had additional complications in that the measured density history in the nozzle was markedly different from that predicted theoretically. In any case a reanalysis of the data would require more information than is available. The error in the data analysis will presumably be smallest closest to the nozzle throat or conversely at the highest temperature at which the rate was deduced. This corresponds to an attachment rate of 4×10^{-31} cm^6 sec^{-1} at 2800°K where the stabilizing partners are a combination of O, O_2, NO, and N_2.

More recently Modica[10] has measured electron production histories in Ar–air and Ar–air–SF_6 mixtures behind reflected shock waves using microwave techniques. In this study the SF_6 was predicted to be completely decomposed to elemental fluorine, and the electron density history in the Ar–air–SF_6 was found to be depressed below that of the equivalent Ar–air observations. The experimental observations were adequately represented by a kinetic scheme which included three-body attachment to fluorine atoms with a rate constant varying monotonically from 4.9×10^{-31} to 3.2×10^{-31} cm^6 sec^{-1} over the temperature range 3700–4500°K. Unfortunately, a sensitivity analysis on the choice of the attachment rate constant was not performed, and since the theoretical predictions are strongly dependent on the air kinetics used it is not possible to comment on the reliability of this result.

Lastly, using a novel experimental technique, Debiesse et al.[11] have deduced a lower bound for the cross section for electron attachment to bromine atoms. In this work copper electrodes were placed on either side of a methane flame. A jet of bromine atoms was then introduced near one of the electrodes and as the electron attachment near the electrode increased a voltage drop was produced across the electrodes. Furthermore, when the electrodes were short circuited, a current produced by the electromotive force resulting from this change in potential could be measured. The voltage and current were measured vs. bromine flow, and a saturation point, corresponding to full attachment, was observed. The electron density was deduced from the measured current, and a lower bound for the attachment rate constant was obtained from the observation that the attachment rate must be more rapid than the recombination rate at saturation.

Debiesse et al. assumed that the attachment process was radiative, i.e.

$$e + Br \rightarrow Br^- + h\nu \qquad (7)$$

and determined that their measurements indicated that the cross section for this process was $>10^{-21}$ cm^2. The accepted cross section for this process, as determined by detailed balancing of the photodetachment cross section,[12] is close to an order of magnitude smaller than this value. Thus if the data of Debiesse et al. are correct, their cross section must correspond to the three-body process and would imply that the attachment rate is greater than 0.8×10^{-32} cm^6 sec^{-1} at 2000°K.

In the last few years several studies of collisional detachment of the halogen negative ions have been performed under conditions where the electron and translation temperatures were equal. In these experiments[13-19] the halogen negative ions are typically created in large excess by the dissociative ionization of shock-heated alkali halide molecules. The resulting temporal behavior of the negative ions and electrons can then be monitored by various means. (For example, in the case of Mandl's experiments[14-18] those quantities are monitored via absorption and emission spectroscopy respectively.)

In most cases the deduced collisional detachment rates, measured over a typical temperature range of 3000–6000°K, could be fit to the simple Arrhenius expression

$$k_d = Ae^{-EA/RT} \quad (8)$$

where EA is the electron affinity of the respective halogen atom. The results of these experiments may be converted to their respective three-body attachment rates by the use of detailed balancing. The equilibrium constant for reaction 2 for an atomic attaching species X is given by

$$K = k_a/k_d = \frac{g_{X^-}}{g_e g_X}\left(\frac{2\pi m_e kT}{h^2}\right)^{-3/2} e^{EA_X/RT} \quad (9)$$

where g_i is the electronic state degeneracy for species i and m_e is the mass of the electron. The resulting values of the attachment rate constant are listed in Table II. In the case of fluorine and chlorine the ground-state degeneracies were adjusted to take into account the effect of low-lying electronic states. In the case of F^-, the magnitude of the detachment rate was found to vary strongly with collision partner. Such a behavior is typical for detachment processes in general, and similar results would be expected for the other halogens. It is noted that Good's[9] value for attachment to F at 2800°K is at least an order of magnitude greater than that predicted from detailed balancing of Mandl's results. It appears that Mandl's value should be preferred given the uncertainty in the data interpretation of the former experiment.

There are no available experimental data on thermal equilibrium electron attachment (or detachment) involving oxygen and hydrogen atoms. The value listed for hydrogen was deduced by Chibisov[6] who applied the principle of microscopic reversibility to the available detachment cross-section data. This value is not Maxwellian averaged and is only valid for the case when the electron and H^- kinetic energy are approximately 0.75 eV. Frommhold[20] has measured the O^- detachment cross section at ion energies greater than 2.25 eV with O_2 as the collisional partner. However, his measurements are not considered sufficiently detailed to warrant determination of the thermal attachment rate constant via microscopic reversibility.

The value listed in Table II for attachment to oxygen atoms was predicted from the modified phase space theory of Shui and Keck.[8] It was assumed that the parameter which describes the O^-–M interaction potential was such that the attachment process required no activation energy. There is, of course, no theoretical justification for this assumption, and the listed rate constant should only be considered as representative.

B. Diatomics

In the case of diatomic molecules, process 2 has been modeled by a modified Bloch–Bradbury[21] mechanism proposed by Herzenberg.[22,23] The mechanism suggested involves the resonant capture of an electron in a two-body reaction resulting in the creation of a negative ion in a vibrationally excited state. The excited ion may then autodetach or be collisionally stabilized. Thus for excitation to a given vibrational level one has

$$e + AB \underset{\tau}{\overset{k_{10}}{\rightleftharpoons}} AB^{-*} \quad (10)$$

$$AB^{-*} + M \xrightarrow{k_{11}} AB^- + M \quad (11)$$

To simplify the analysis one can assume that AB^{-*} is created preferentially in one excited state and then, by making the steady-state approximation for AB^{-*}, one can write the overall three-body attachment rate as

$$k_a = k_{10}k_{11}/(\tau^{-1} + k_{11}N) \quad (12)$$

where N is the total number density. The above expression reduces to

$$k_a \approx k_{10}k_{11}\tau \quad (13)$$

when $\tau^{-1} > k_{11}N$.

This type of analysis can explain the observed increase in attachment rate constant with increasing complexity of the stabilizing partner (see Table II) since molecules with more degrees of freedom would be expected to be more readily able to absorb the excess energy of AB^{-*} in a stabilizing collision.

In the more formal analysis of Herzenberg[22] the initial electron capture is pictured to proceed via excitation to a resonant state, and the capture cross section is described in the Breit–Wigner formalism.[24] For capture of an electron of energy E by a molecule, initially in the state a, creating a negative ion excited to vibrational level n the cross section is given by

$$\sigma_c^n(a;E) = \pi\lambda^2(C^n/g)\{\Gamma_a^n\Gamma^n/[(E - E_n)^2 + (\tfrac{1}{2}\Gamma^n)^2]\} \quad (14)$$

where C^n is the number of degenerate resonances corresponding to level n, g is the total number of spin states of the collision partners e and AB, λ is the deBroglie wavelength of the electron, Γ_a^n is the partial width of the resonance from state a to n, Γ^n is the total width from all states a, and E_n is the energy at which the resonance occurs. The total capture rate constant for molecules in initial state a is

$$k_c = \sum_n \int dE\, \sigma_c^n(a;E)\, V_e(E) F_e(E) \quad (15)$$

where V_e is the electron velocity and F_e is the Maxwell–Boltzmann distribution function. Under the assumption that the radiative lifetime of the resonance

$$\tau_n = \hbar/\Gamma^n \quad (16)$$

is shorter than the stabilization time, τ_c, the percentage of these excited ions which are stabilizied, is τ_n/τ_c. Herzenberg has defined τ_c in terms of the Langevin cross section (eq 1), i.e.

$$\tau_c^{-1} = 2\pi\zeta e(\alpha/\mu)^{1/2}N \quad (17)$$

where ζ is the probability that the collision will be a stabilizing one.

The overall attachment rate for molecules AB initially in state a is then (for $\tau_n < \tau_c$)

$$k_a = 2\pi\zeta e\left(\frac{\alpha}{\mu}\right)^{1/2}\left(\sum_n \tau_n \int dE \sigma_c^n(a;E) V_e(E) F_e(E)\right) \quad (18)$$

Note that if the width of $F_e(E)$ is broad compared with Γ^n, then the quantity $F_e V_e$ may be taken out of the integral with the result

$$k_a = \left(\frac{4\pi^3\hbar^2 e}{m_e}\right)\left(\frac{\alpha}{\mu}\right)^{1/2}\zeta\left[\sum_n F_e(E_n)(C^n/g) \times \lambda(E_n)(\Gamma_a^n/\Gamma^n)\right] \quad (19)$$

One sees that the width of the resonance only appears as a ratio in expression 19. This result markedly simplifies the evaluation of the attachment rate constant; in particular, for the lowest resonance there is usually only one channel available in which case $\Gamma_a^n/\Gamma^n = 1$.

For the case of oxygen molecules, discussed below, Herzenberg[22] used the vibrational excitation cross sections of Hake and Phelps[25] to make a rough estimate of the partial width of the lowest resonance, $\Gamma_{a_0}^n$, where a_0 refers to the ground vibrational state of O_2, and deduced a value of 2×10^{-6} eV. Very recently Koike and Watanabe[26] have developed an ab initio derivation for the initial capture cross sec-

TABLE II. Direct Electron Attachment to Atoms and Molecules

$$e + A + M \xrightarrow{k} A^- + M$$

$$\Delta H_{f\,298} = -E.A.(A) - 0.064\ eV$$

REACTION	M	k, cm^6-sec	T, °K	P_M, Torr	REF.	COMMENTS
1) $e + Br + M \rightarrow Br^- + M$	Ar	1.6×10^{-32}	3960	> 760	13 e, i	
	Ar	$3.3 \times 10^{-30} (\frac{300}{T})^{3/2}$	2700 - 4300	" "	19 e, i	
	CH_4 Flame Products	$> 8. \times 10^{-33}$	2000	760	11 f	See Text
2) $e + Cl + M \rightarrow Cl^- + M$	Ar	1.4×10^{-31}	3200	-	19 e, i	See Also Ref. 15
3) $e + F + M \rightarrow F^- + M$	Ar	$1.6 \times 10^{-31} (\frac{300}{T})^{3/2}$	4000 - 6000	> 760	14 e, i	
	Ar	$5.3 \times 10^{-32} (\frac{300}{T})^{3/2}$	3600 - 7200	" "	19 e, i	
	CO	$2.3 \times 10^{-30} (\frac{300}{T})^{3/2}$	3600 - 5300	" "	17 e, i	
	N_2	$8.0 \times 10^{-31} (\frac{300}{T})^{3/2}$	3000 - 5400	" "	15 e, i	
	Shock Heated Air	$\sim 4 \times 10^{-31}$	2800	~1000	9 e	See Text
	Shock Heated Air-Ar	$1.4 \times 10^{-30} (\frac{300}{T})\, e^{(5390/T)}$	3700-4500	~760	10 e	See Text
4) $e + H + M \rightarrow H^- + M$	H	3×10^{-32}	$E_e \sim 0.75$ eV	-	6 i	Not Maxwell Averaged, See Text.
5) $e + I + M \rightarrow I^- + M$	Ar	$< 5 \times 10^{-31}$	2400	> 760	19 e, i	
	Ar	$7 \times 10^{-31} (\frac{300}{T})^{3/2}$	3800 - 6000	" "	18 e, i	
	N_2	$1.2 \times 10^{-30} (\frac{300}{T})^{3/2}$		" "	18 e, i	
6) $e + O + M \rightarrow O^- + M$	Ar	$1.0 \times 10^{-30} (\frac{300}{T})$		-	8 h	See Text
7) $e + Br_2 + M \rightarrow Br_2^- + M$	He	$< 5 \times 10^{-31}$	296	50	75 b	Deduced from Diss. Att. Data
8) $e + HCl + M \rightarrow$?	HCl					See Text
9) $e + I_2 + M \rightarrow I_2^- + M$	He	$< 2.5 \times 10^{-28}$	296	20	73 b, 74 b	Deduced from Diss. Att. Data
10) $e + NO + M \rightarrow NO^- + M$	Ar	$< 10^{-33}$	285	0.4	65 c, i	
	He	$2.5 \times 10^{-31} (\frac{300}{T})^{3/2} e^{(\frac{590}{T})}$	200 - 500	"	62 c, i	Uncertainty ± 10 - 50% (Rate listed incorrectly in Ref. 62)
	Ne	$6.9 \times 10^{-32} (\frac{300}{T})^{3/2} e^{(-\frac{860}{T})}$	" "	"	" "	Uncertainty ± 10 - 50%
	CO	$1.6 \times 10^{-31} (\frac{300}{T})^{3/2} e^{(-\frac{250}{T})}$	" "	"	" "	"
	H_2	$3 \times 10^{-31} (\frac{300}{T})^{3/2} e^{(-\frac{680}{T})}$	" "	"	" "	"
	NO	$1.5 \times 10^{-29} (\frac{300}{T})^{3/2} e^{(-\frac{940}{T})}$	" "	"	" "	"
		$(8 \pm 2.) \times 10^{-31}$	300	2-3, 60-160	63 a, g, i	See Fig. 3
		$(5.9 \pm 1.2) \times 10^{-31}$	300	"	63 a, g, i	
	CO_2	$1.0 \times 10^{-29} (\frac{300}{T})^{3/2} e^{(-\frac{660}{T})}$	200 - 500	0.4	62 c, i	Uncertainty ● 10 - 50%
		$(1.1 \pm .24) \times 10^{-30}$	300	0.4 - 2.3	64 a, g, i	
	N_2O	$2 \times 10^{-29} (\frac{300}{T})^{3/2} e^{(-\frac{970}{T})}$	200 - 500	.4	62 c, i	Uncertainty ± 10 - 50%
		$(7.1 \pm 1.2) \times 10^{-31}$	300	0.4 - 2.9	64 a, g, i	
	NH_3	$1. \times 10^{-29} (\frac{300}{T})^{3/2} e^{(-\frac{410}{T})}$	200 - 500	0.4	62 c, i	Uncertainty ● 10 - 50%
11) $e + OH + M \rightarrow OH^- + M$	-	$\sim 10^{-30}$	2000	-	70 f	Est. See Text
12) $e + O_2 + M \rightarrow O_2^- + M$	He	$(7.5 \pm .8) \times 10^{-32}$	300	-	30 b	
		2.5×10^{-32}	"	-	32 a	
	N_2	$(1.1 \pm .1) \times 10^{-31}$	"	-	30 b	
		3.5×10^{-32}	"	10	31 b	Extrap.
		$(1 \pm .5) \times 10^{-31}$ *	300 - 500	-	28a, 32a, 36a	
		2.6×10^{-31}	300	10 - 100	33 c	Continuous Irradiation
		$(1.6 \pm 0.8) \times 10^{-31}$	"	.6 - 8	37 c, g	As deduced from their Air and O_2 Meas.
		$\sim 1.5 \times 10^{-31}$	"	300 - 1500	43 a, b	Some Press. Effects Observed. See Text

TABLE II (*Continued*)

REACTION	M	k, cm^6 -sec	T, °K	P_M, Torr	REF	COMMENTS
12 Cont'd.) $e + O_2 + M \rightarrow O_2^- + M$	NO	Sim. to O_2	300	1.2	63 a, g	
	O_2	$(2.1 \pm 0.2) \times 10^{-30}$	"	1 - 150	30 b	
		2.4×10^{-30}	"	0.5 - 2.	31 b	
		$(1.4 \pm 0.2) \times 10^{-29}\left(\frac{300}{T}\right) e\left(-\frac{600}{T}\right)$	195 - 600	7.6 - 54	28a, 32a, 36a	See Fig. 2
		1.7×10^{-30}	300	10 - 100	33 c	Continuous Irradiation
		$(2.12 \pm 0.14) \times 10^{-30}$	"	1 - 10	37 c, g	
		$(1.9 \pm 0.3) \times 10^{-30}$	130	1 - 20	40 b	
		$(1.4 \pm 0.2) \times 10^{-30}$	210	"	"	
		$(2.05 \pm 0.1) \times 10^{-30}$	280	"	"	
		$(2.6 \pm 0.3) \times 10^{-30}$	465	"	"	
		$(3.3 \pm 0.9) \times 10^{-30}$	575	"	"	
		$(2.2 \pm 0.1) \times 10^{-30}$	296	3 - 100	39 b	
		2.5×10^{-30}	300	0.5 - 10	43 a, b, i	Extrap. from $<e> = 0.042$ eV
		$(4. \pm 0.3) \times 10^{-30} e\left(-\frac{196}{T}*\right)$	113 - 300	0.9 - 5	42 b, g	See Text & Fig. 2
		$2.2 \times 10^{-29} \left(\frac{300}{T}\right)^{3/2} e\left(-\frac{900}{T}*\right)$	>300		This survey	" "
	CO_2	$(3.3 \pm 0.7) \times 10^{-30}$ *	300 - 525	4.3 - 700	28a, 34a, 36a	
		3.2×10^{-30}	300	-	38 a	
		$(3.0 \pm 0.2) \times 10^{-30}$	296	3 - 187	39 b	
	H_2O	$(1.4 \pm 0.2) \times 10^{-29}$	300 - 400	3.1 - 11	34 a, 36 a	
		$(1.4 \pm 0.5) \times 10^{-29}$	300	1.25 - 18	35 a	
		1.38×10^{-29}	300	-	38 a	
	C_2H_4	$(3.4 \pm 0.4) \times 10^{-30}$	300	200 - 800	35 a	
		2.5×10^{-30}	300	40 - 80	38 a	
13) $e + CO_2 + M \rightarrow CO_2^- + M$	CO_2	$< 6 \times 10^{-36}$	300	-	80 a	
14) $e + H_2O + M \rightarrow H_2O^- + M$	H_2O	$< 9 \times 10^{-36}$	300	24.6	87 a	
15) $e + N_2O + M \rightarrow$? See Text	N_2	$(3 \pm 0.5) \times 10^{-33}$	300	400 - 900	91 a, j	Extrap. from $<e> = 0.18$ eV
		5.4×10^{-34}	300	35 - 190	92 b	k_{eff} . See Text
	N_2O	$(6 \pm 1.) \times 10^{-33}$	300	30 - 191	88 a	" "
		$\sim 3 \times 10^{-33}$	195	-		
		$(5.6 \pm 0.2) \times 10^{-33}$	300	10 - 200	89 b	" "
		$(4.3 \pm 0.6) \times 10^{-33}$	"	4 - 28	92 b	" "
16) $e + NO_2 (+M) \rightarrow NO_2^- (+M)$	Ar	4.5×10^{-11}	300	3 - 70	95 b	k in cm^3 -sec^{-1}
	He	5×10^{-11}	"	10 - 100	96 b	Data re-interpreted k in cm^3 -sec^{-1}
		2×10^{-11}	"	3 - 70	95 b	k in cm^3 -sec^{-1}
	Kr	3×10^{-11}	"	"	"	"
	Ne	3.1×10^{-11}	"	"	"	"
	Xe	2.5×10^{-11}	"	"	"	"
		$(1.1 \pm 0.3) \times 10^{-12}$	"	8.8 - 15.9	97 b	"
	N_2	4.0×10^{-11}	"	3 - 70	95 b	"
		$(1.1 \pm 0.3) \times 10^{-12}$	"	6.3 - 20.5	97 b	"
	NO	$\left(1.4^{+0.2}_{-0.9}\right) \times 10^{-11}$	"	0.2 - 0.7	61 b, g	"
	CO_2	1.8×10^{-10}	"	-	38 a	"
	NO_2	1.6×10^{-27}	"	0.03 - 0.15	96 b	
		1.1×10^{-10}	"	0.15 - 0.9	"	Data re-interpreted k in cm^3 - sec^{-1}
17) $e + O_3 + M \rightarrow O_3^- + M$	CO_2	$< 10^{-30}$	"	10 - 100	93 a	Deduced from Diss. Att. Data
18) $e + SO_2 (+M) \rightarrow SO_2^- (+M)$	N_2	$(6.6 \pm 0.6) \times 10^{-12}$	300	10 - 160	99 a	k in cm^3 - sec^{-1}
	CO_2	$\sim 6 \times 10^{-30}$	"	3 - 160	"	
	SO_2	$(3.5 \pm 0.6) \times 10^{-12}$	"	0.8 - 3.2	"	k in cm^3 - sec^{-1}

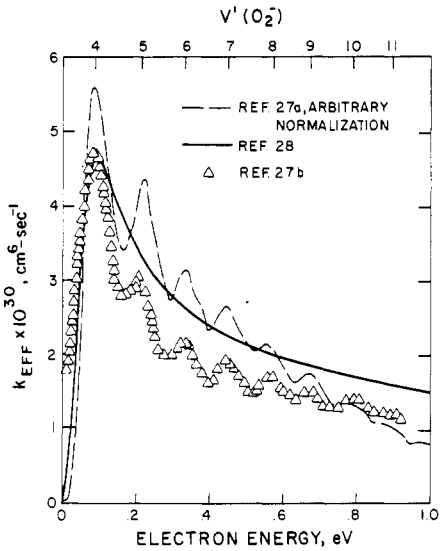

Figure 1. The rate constant for the reaction e + O_2 + O_2 → O_2^- + O_2 vs. electron energy. The symbols correspond to a theoretical prediction while the solid and dashed lines are experimental data. The data of ref 28 are plotted vs. "mean" electron energy.

tion for O_2. Their result is easily reduced to the one level Breit–Wigner formula, and furthermore the resonance widths are expressed in terms of matrix elements which may be evaluated directly. Their theoretical prediction for the width of the lowest resonance is 4×10^{-6} eV. Thus it would appear that at least for the lowest resonance in O_2 the approximation which leads to expression 19 is quite reasonable. Furthermore, this resonance width corresponds to an autodetachment lifetime of order 10^{-10} sec which in turn may be used to define the range over which attachment to O_2 should have a three-body pressure dependence.

The remainder of this section is concerned with a review of the available data on electron attachment to diatomic molecules. The data base is summarized in Table II. Comparisons between the experimental data and theoretical predictions will be made where possible.

1. O_2

a. The Data Base

The process of thermal electron attachment to the oxygen molecule has been studied by a large number of experimentalists[27-46] for a variety of third bodies and is perhaps the best documented of all negative ion reactions. The experimental methods used generally fall into two categories: (a) drift tube techniques and (b) stationary afterglows. As can be seen by reference to Table II, the rate constant has a strong dependence on the nature of the third body, the trend being that the larger the third body the larger the rate constant.

Note that the rate constant for M = O_2 is much larger than that for M = N_2. It has been suggested[32] that this may result because stabilization by O_2 could occur via a charge-transfer reaction

$$(O_2^-)_1^* + (O_2)_2 \rightarrow (O_2^-)_2 + (O_2)_1 \qquad (20)$$

Other mechanisms[47,48] involving electronic state transitions have also been postulated to explain the large stabilization efficiency of oxygen molecules.

b. Electron Energy Dependence

The validity of Herzenberg's analysis, as applied to attachment to the oxygen molecule, has recently been clearly verified in the temperature range 300–800°K by the experimental study of Spence and Schulz.[27a] In this work a high-resolution electron beam, with half-width of ≈100 meV, was used to measure the cross section for electron attachment to oxygen in the electron energy range of 0–1 eV. The cross section was observed to rise from zero to a peak at an electron energy corresponding to the fourth vibrational level of O_2^- (the lowest resonance) and then to have additional peaks at energies corresponding to the higher vibrational levels of O_2^-. The results of this experiment at 300°K are shown in Figure 1 along with the drift tube measurements of Pack and Phelps[28] and a prediction by Chapman and Herzenberg.[27b] As can be seen, the agreement between the three is excellent. (It should be noted that the measurements of Pack and Phelps were performed in a drift tube, and thus the energy scale for their data corresponds to a "mean" electron energy deduced under the assumption that the electron velocity distribution is Maxwellian.) The rate constant data plotted in Figure 1 are an effective three-body coefficient

$$k(E) = \sigma(E)v(E) \qquad (21)$$

where E is the electron energy, σ the cross section, and v the electron velocity.

The Chapman–Herzenberg prediction shown, based on the modified Bloch–Bradbury mechanism as illustrated by eq 10 and 11, was evaluated from a modified version of eq 18. The Maxwellian electron distribution function has been replaced with a Gaussian distribution with half-width of 110 meV, in line with the electron distribution in Spence and Schulz's experiment. Only transitions from the ground vibrational state of oxygen were considered, and ζ, the stabilizing probability, was taken to be unity.

c. Pressure Dependence

At room temperature, transitions involving vibrationally excited O_2 are relatively unimportant, and the dominant contribution to the thermally averaged rate will be the $v' = 4$ resonance, and thus the simpler mechanism which results in relationships 12 and 13 may be used in examining the experimental data. Attachment to oxygen molecules with O_2 as the stabilizing partner has been demonstrated to manifest a P^2 dependence up to pressures of 150 Torr[30] at room temperature. This result may be used to deduce an experimental lower bound of 1.0×10^{-11} cm^3 sec^{-1} for k_{10} since this rate cannot be smaller than the "effective" two-body attachment coefficient, $k_a N$. This value is two-thirds of Herzenberg's prediction, as defined by eq 15, for a resonance energy of 79 meV (see below) and a resonance width of 4×10^{-6} eV.[26] Thus, given the validity of Herzenberg's analysis, electron attachment to O_2 should become a saturated three-body reaction at ~225 Torr for the collision partner O_2 and ~150 Torr for the collision partner CO_2. The saturation pressure is, of course, linearly proportional to the resonance width, and thus the validity of the above assertion depends upon the accuracy to which that latter quantity is known. Indeed, attachment to O_2 with CO_2 as a stabilizing partner has been shown to scale as P^2 up to 700 Torr in one drift tube study[28] and conversely has been found to diverge from a P^2 dependence at pressures above 220 Torr in another.[29]

Furthermore, McCorkle et al.,[43] in a drift tube experiment, have studied three-body attachment to O_2, with N_2 as a stabilizing partner, over a pressure range of 300–10,000 Torr. The monoenergetic attachment cross sections were deduced from their data by a swarm unfolding technique.[49] In the pressure range of 300–500 Torr the sharp resonance peak, corresponding to the fourth vibrational level of O_2^-, was observed; however, at the higher pressures it disappeared and the peak cross section gradually shifted toward thermal energy with increasing nitrogen pressure.

It is interesting that the observed attachment rate in this work showed virtually no deviation from a three-body pressure dependence up to 7000 Torr (except for a small kink at about 500 Torr). McCorkle et al. determined that the resonance width, Γ^4, was $>4.9 \times 10^{-6}$ eV, at 7000 Torr, corresponding to a lifetime, $\tau(O_2^{-*}) < 1.3 \times 10^{-10}$ sec. The stabilizing probability for N_2, ζ_{N_2}, has been found to be 0.03 (see Table II); thus the time between stabilizing collisions at 7000 Torr would be 1.3×10^{-10} sec, and therefore the start of saturation should have been observed. The authors suggest that either $\tau(O_2^{-*})$ is much less than 1.3×10^{-10} sec or that the N_2 is involved in "sticky," as well as stabilizing, collisions; i.e., the N_2 perturbs, through "sticky" collisions, the O_2^- potential curve with a net downward shift. This effect becomes more pronounced with increasing N_2 density. It should be emphasized that the resonance peak corresponding to O_2^- ($v = 4$) was not observed in the cross-section data at 7000 Torr, and thus the "resonance width" deduced from the cross-section data taken at this pressure may not be meaningful.

Recently Christophorou[44] has suggested a kinetic scheme, involving both stabilizing and "sticky" collisions, to explain the observations of McCorkle et al.[43] The lifetime of O_2^{-*} was determined to be $<4 \times 10^{-12}$ sec from this analysis. The key reaction in determining the lifetime of O_2^{-*} in this scheme was collisional detachment of O_2^{-*}. It has been suggested[50] that if this reaction is included in an attachment scheme the reverse reaction must also be included. If this is done, Christophorou's scheme no longer explains the data (see the discussion on direct attachment to NO_2). If both these reactions are excluded, the upper bound on the lifetime of O_2^{-*} becomes 1.3×10^{-10} sec, again determined at 7000 Torr.

Goans and Christophorou have also studied attachment to O_2 highly diluted in ethylene for pressures up to 18,000 Torr.[45] From the analysis of these data, which required postulating only the capture and stabilization reactions 10 and 11, he deduced the lifetime of O_2^{-*} to be 2×10^{-12} sec, appreciably lower than the estimates of Herzenberg[22] and of Koike and Watanabe.[26] Thus the work of Christophorou and coworkers seems to indicate that there are fundamental differences between attachment processes occurring at high and at low pressures. A definitive determination of the resonance energy width of O_2^{-*} would be of great value in understanding these observations.

d. Temperature Dependence

The temperature dependence of the rate constant for attachment to O_2 has been studied over a limited range for the stabilizing partners O_2, N_2, CO_2, and H_2O. The largest data base is for O_2 and is shown in Figure 2. The dashed line in the figure is the rate estimation of Phelps,[36] i.e.

$$k_{a,O_2} = 1.4 \times 10^{-29}(300/T)e^{-600/T} \text{ cm}^6 \text{ sec}^{-1} \quad (22)$$

Although the Herzenberg theory[22] involves a series of resonances, each with a distinct activation energy, it may be roughly characterized for low temperatures with the activation energy of the lowest resonance. This corresponds to the fourth vibrational level of the O_2^- ($X^2\Pi_{3/2}$) state which has recently been shown by Land and Raith[51] to lie 79 meV above the ground state of O_2. This value is in good agreement with other recent determinations.[52-54] A direct evaluation of eq 19 for this resonance energy, with $\zeta = 1$ and $C^n = 4$, $g = 6$, as suggested by Herzenberg,[22] results in the attachment rate constant expression

$$k_{a,O_2} = 4.2 \times 10^{-29}(300/T)^{3/2}e^{-900/T} \quad (23)$$

This rate is shown as the dash–dot line in Figure 2 and is little different from the Phelps value in the temperature range plotted. Choosing this form for the attachment rate, the low-temperature detachment rate becomes

$$k_{d,O_2} = 7.7 \times 10^{-10}e^{-6000/T} \quad (24)$$

This value is in excellent agreement with the data[28] and, as expected since $\zeta = 1$, the frequency factor is just the "orbiting" rate constant, eq 1.

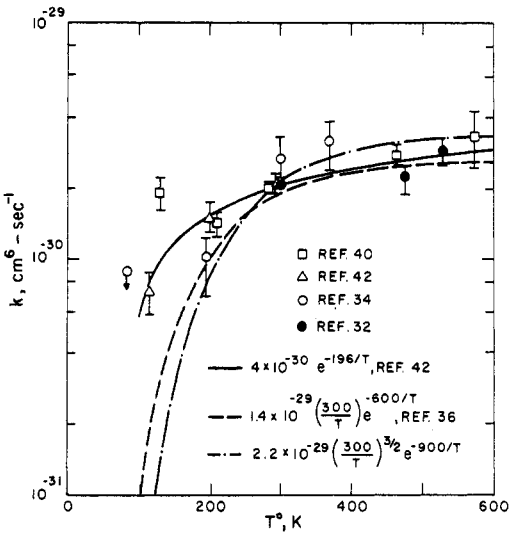

Figure 2. The rate constant for the reaction $e + O_2 + O_2 \rightarrow O_2^- + O_2$ vs. gas temperature.

It is noted that both of the rates listed above provide values below 300°K much lower than that observed in the experimental work of Truby[42] and Van Lint et al.[40] Their results cannot be explained in terms of the resonance theory discussed above. Truby[42] has suggested that the low-temperature data may be due to dissociative attachment of the dimer O_4, i.e.

$$e + O_4 \rightarrow O_2^- + O_2 \quad (25)$$

Such a process would still exhibit a three-body pressure dependence since the dimer's concentration would scale as the square of pressure. The dimer has recently[55,56] been observed at low temperatures and has been assigned a bond strength of 0.53 kcal/mol. It may be that the dimer thermochemistry is such that its formation is much more highly favored at 100°K than at 300°K so that the dimer's effect on the overall attachment rate would only be important at the lower temperature. For example, a crude estimate of the partition function for O_4, assuming the molecule to be nonlinear, would suggest that the ratio of $[O_4]/[O_2]^2$ could decrease by a factor of 50 between 100 and 300°K.

It can be seen that Truby's expression for k_{a,O_2}, shown as the solid line on Figure 2, is the best fit of the data between 100 and 600°K and should be preferred for low-temperature applications. For applications involving temperatures greater than 300°K, the rate formulation 23 is recommended since it is in agreement with theory as well as the data. Of course it is not clear that the temperature dependence listed in relationship 23 will hold at higher temperatures where transitions from vibrationally excited states of O_2, as well as those involving higher resonances, begin to be important. If one assumed that the rate for detachment given by eq 24 is valid at higher temperatures, then microscopic reversibility using the detailed equilibrium constant would imply that the rate constant representation 23 would be valid up to temperatures of at least 2000°K. However, reference must be made to the recent work of Freeman et al.[46] who examined the electron capture coefficient for attachment of oxygen molecules in the temperature range of 350–825°K. In this work they observed

a variation in the rate constant temperature dependence which they explain by proposing an additional electron capture mechanism resulting in the creation of a stable excited state of the ion, the O_2^- ($^2\Sigma_g$) state, with an activation energy of 1.04 ± 0.22 eV.

e. Overview

As mentioned earlier the process of three-body electron attachment to oxygen molecules is perhaps the most studied of all electron attachment processes, and yet the data base exhibits a number of conflicting features.

The work of Spence and Schulz[27a] validates Herzenberg's[22] picture of electron attachment in O_2 occurring via a discrete series of resonant states. Furthermore, for pure O_2, the data base for temperatures between 250 and 600°K is quite adequately represented by the theory with the only adjustable parameter ζ set to unity. Below 250°K the data fall more slowly than the theory; however, this may be due to the advent of an additional reaction, eq 25. Additional studies of both low-temperature attachment to oxygen molecules and the thermochemical properties of O_4 would be of value in understanding this phenomenon.

The most perplexing feature of the data base relates to the pressure dependence of the attachment process. Herzenberg's analysis would imply that pressure saturation should occur at a given pressure dependent upon the stabilization efficiency of the collision partner. A number of drift tube experiments[43-45] have shown that saturation does not occur at the predicted pressure. These results may be interpreted to imply that the lifetime of the resonant state is much shorter than anticipated,[22,26] or that the lifetime is a function of foreign gas pressure.

It should be emphasized that the analysis of high-pressure drift tube measurements can be quite complicated. For example, Grunberg[29] examined the pressure dependence of attachment in pure O_2 for electron energies somewhat above thermal and found that the apparent attachment rate faltered from a P^2 dependence at pressures as low as 66 Torr. Upon analysis of his data he found that this was not due to pressure saturation but rather to the fact that attachment was proceeding so rapidly that the electron energy distribution could not replenish itself; i.e., in an attaching gas such as O_2 the electron energy distribution in a drift tube is determined by the same type of collisions as provide attachment.

This particular phenomenon did not occur in the studies of Christophorou and coworkers[43-45] since their measurements were performed in O_2 strongly diluted in a nonattaching gas. Their studies have raised serious questions concerning a fundamental attachment process at high pressures. It is clear that a more precise definition of the resonance widths must come from electron scattering experiments and their like rather than high-pressure drift tube measurements. (For example, in a scattering experiment, Linder and Schmidt[53] recently determined the lifetime of the O_2^- (v = 9) resonance to be $\sim 10^{-12}$ sec, in good agreement with the prediction of Koike and Watanabe.[26]) It is just as clear that such measurements should not be blindly applied to high-pressure conditions where effects such as the "sticky" collision phenomenon suggested by Christophorou and coworkers may occur.

2. NO

a. The Data Base

Thermal electron attachment to NO has also been studied in a number of experiments,[38,46,57-65] and an apparent three-body attachment process has been observed over the pressure range of 0.2 to 160 Torr. However, in the majority of experiments,[46,57-61] the deduced attachment rate was incorrect

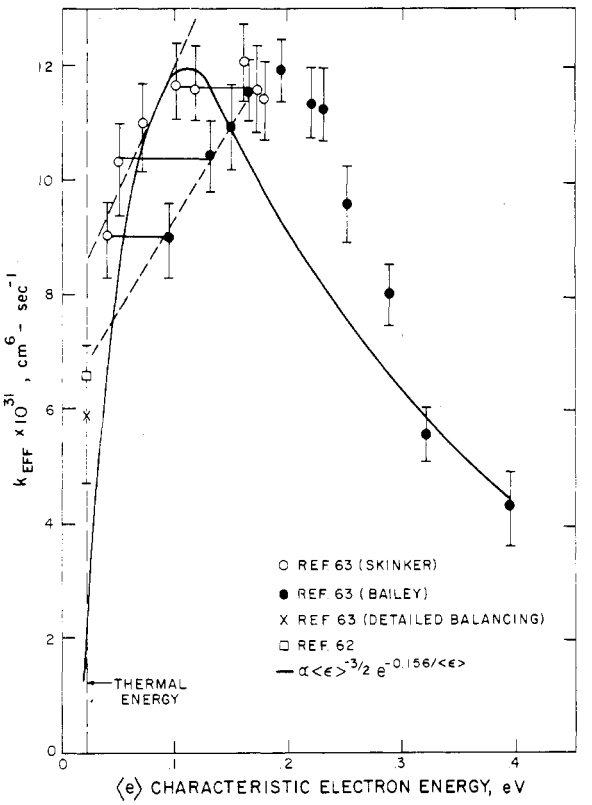

Figure 3. The rate constant for the reaction e + NO + NO → NO^- + NO vs. characteristic electron energy.

since the effects of detachment and clustering processes were not considered. The inclusion of these processes has been shown[62,63] to be of fundamental importance in the analysis of attachment data in pure NO. The only reported unambiguous measurements are those of Parkes and Sugden,[63] made in a drift tube with mass filter at pressures of ~2–3 and ~60–160 Torr, and the collisional detachment measurements of McFarland et al.[62] The high-pressure results of Parkes' experiment are shown in Figure 3 where the attachment rate is plotted vs. the characteristic electron energy, $\langle\epsilon\rangle$ (this quantity is equivalent to kT_e if the electron distribution is Maxwellian). There is some uncertainty in the relationship between the reduced field and the characteristic energy for NO at low energies. The attachment coefficient is plotted using both the $\langle\epsilon\rangle$ vs. reduced field data of Bailey and Somerville[66] and of Skinker and White.[67] Parkes and Sugden suggest that Bailey's values should be preferred. The linear extrapolation used is based both upon the comparison between the high- and low-pressure results of ref 63 as well as the flowing afterglow measurements of the reverse reaction. The value of the attachment coefficient as determined by detailed balancing of the detachment measurements of McFarland et al.[62] and by Parkes and Sugden are also shown for comparison. (In the evaluation of the equilibrium constant the electron affinity of NO was taken to be 24 meV in accord with the observations of Siegel et al.[68])

b. Data Reanalysis

Earlier measurements[38,57-61] of the room-temperature attachment rate in pure NO were up to an order of magnitude lower than those shown in Figure 3. Parkes and Sugden have pointed out that a sequence of three reactions are important in analyzing attachment data in pure NO, these being

$$e + NO + NO \underset{k_{-26}}{\overset{k_{26}}{\rightleftarrows}} NO^- + NO \qquad (26)$$

$$NO^- + 2NO \xrightarrow{k_{27}} \text{stable ions} \qquad (27)$$

TABLE III. Reanalysis of Electron Attachment Data for NO (T = 300°K)

$$e + NO + NO \xrightarrow{k} NO^- + NO$$

k_{eff}, cm^6 sec^{-1} × 10^{31}	NO, parts/cc	k, cm^6 sec^{-1} × 10^{31}	Ref
4	1.4–5.6 × 10^{17}	11.5	57, b
2.2–3.3	1–5 × 10^{17}	8.8	58, b, g
1.3	0.75–1.9 × 10^{17}	7.8	59, b
2.2	1.4 × 10^{17}	12.5	60, b
2.2	3.8–10 × 10^{17}	4.3	38, a, j
0.68	0.75–2.1 × 10^{16}	32	61, b, g
		6.6	62, c, i
	2.2–5.3 × 10^{18}	8.0	63, a, g, j

where k_{-26} and k_{27} have been measured[63] to be 5 × 10^{-12} cm^3 sec^{-1} and 7.6 × 10^{-30} cm^6 sec^{-1}, respectively. In a system without diffusive effects and where recombination is not important, the governing differential equations become

$$d[NO^-]/dt = k_{26}[e][NO]^2 - k_{-26}[NO^-][NO] - k_{27}[NO^-][NO]^2. \quad (28)$$

$$d[e]/dt = -k_{26}[e][NO]^2 + k_{-26}[NO^-][NO] \quad (29)$$

where the bracketed quantities are number densities. Making the steady-state assumption for NO^- results in

$$d[e]/dt = -k_{27}\frac{k_{26}[e][NO]}{k_{-26} + k_{27}[NO]}[NO]^2 = -k_{eff}[e][NO]^2 \quad (30)$$

where k_{eff} is the quantity measured in the earlier experiments. Thus

$$k_{26} = k_{eff}\frac{k_{-26} + k_{27}[NO]}{k_{27}[NO]} \quad (31)$$

Listed in Table III are the determinations of k_{eff} from various experiments, the NO density range in each experiment, and the value of k_{26} deduced from eq 31 using the values of k_{-26} and k_{27}, as determined by Parkes and Sugden, and the average number density of NO in each experiment. Considering the uncertainties in the various rate constants it is gratifying that all the values of k_{26} so deduced fall in the range 8 ± 4 × 10^{-31} cm^6 sec^{-1} with the exception of that of Puckett et al.,[61] to which the largest correction was applied. (In this latter experiment, the electron decay is not monitored directly, but rather the time of transition from electron–positive ion to negative ion–positive ion ambipolar diffusion is related to the rate constant. This transition occurs at very low electron densities where the steady-state assumption for NO^- is presumably invalid.)

Both McFarland et al.[62] and Parkes and Sugden[63] observed a relatively weak temperature dependence for the attachment rate between 200 and 500°K, whereas the Gunton and Shaw[58] measurements of k_{eff} implied that the rate varied as T^{-3} between 200 and 400°K. The latter observation is consistent with the mechanism described by relationship 31 since at lower (higher) temperatures than 300°K k_{-26} will decrease (increase) and k_{27} will increase (decrease) and thus k_{eff} would be expected to increase (decrease) if k_{26} were relatively constant. Lastly, in those of the above experiments where mass analysis was performed,[58,61,63] the negative ion observed was NO_2^-, rather than NO^-, as would be expected if the reaction sequence (26)–(27) controlled the electron decay. In all then, it appears that attachment in pure NO occurs at a rate of approximately 8 × 10^{-31} cm^6 sec^{-1} at room temperature.

c. Attachment Mechanism

The results of McFarland et al.[62] demonstrate that the NO attachment rate behaves much like that of O_2 in both temperature dependence and relative third-body efficiencies at least for low temperatures. However, the attachment mechanism in this case is not well established. If a mechanism such as (10)–(11) were proposed for attachment to NO, the resonance at NO^- (v = 1) should appear at 0.156 ± 0.040 eV[68] above the ground state of NO. Parkes[63] suggests the expected energy variation of the attachment rate constant should be (see eq 19 in the limit of only one open channel)

$$k_a \propto T_e^{-3/2} e^{-E/kT_e} \quad (32)$$

where T_e is the electron temperature and E is the resonance energy. For NO this would have the shape of the solid curve shown in Figure 3. Here it has been assumed that the electron velocity distribution in the drift tube is Maxwellian and that therefore $\langle \epsilon \rangle = kT_e$. While this form is in qualitative agreement with the data at higher energies, it falls off much too rapidly at lower energies. This observation is in agreement with McFarland's work where the activation energy as determined from detailed balancing of the detachment rate constant is ~0.08 rather than 0.156 eV. Two additional mechanisms which have been suggested to explain the data are dissociative attachment of the dimer, N_2O_2, and direct three-body capture with zero resonance energy. Parkes and Sugden[63] suggest the latter to be more probable since the attachment rate remains relatively constant between 300 and 500°K whereas the dimer concentration would be expected to decrease notably over that temperature range. An additional argument against dissociative attachment to the dimer is that McFarland et al. examined the detachment rate for a variety of detaching partners and found that in all cases the deduced activation energy for attachment was significantly less than 0.156 eV.

It should be pointed out that expression 32 is only valid when $\Gamma_a^n \ll kT$. This is not the case for NO at room temperature where the lowest resonance has been shown to have a width of 0.02 eV[69] and the proper evaluation of eq 18 results in a rate constant whose effective activation energy at low temperatures is less than 0.156 eV and more in line with the observations of Parkes and of McFarland et al.

However, it would appear that Herzenberg's[22] theory should not be applied to NO in any case. In his analysis it is assumed that the time between capture and stabilization is sufficiently large so that the two processes may be considered independent. For the case of attachment to O_2 this is quite reasonable since the lifetime of the resonant state is of order 10^{-10} sec, corresponding to distances of order 10^{-5} cm for thermal velocities. However, in the case of NO the lifetime of the lowest resonance[69] is 3 × 10^{-14} sec, which corresponds to an average distance of ~10^{-9} cm between capture and stabilization. Thus for this case it would appear that a two-stage process cannot occur.

A further complication in analyzing the attachment phenomena in NO is the observation of Freeman et al.[46] that their study of the temperature dependence of the electron

capture coefficient suggests that an additional process occurs, involving an excited state of NO^- with an activation energy of ~0.4 eV.

3. OH

The only other diatomic molecule for which three-body attachment information is available is OH. Calcote and Jensen[70] have pointed out that at temperatures of approximately 2000°K an attachment rate of $\approx 10^{-30}$ cm^6 sec^{-1} would give qualitative agreement with some flame observations and have suggested that the attachment rate for OH may be similar to that for O_2. This estimate is somewhat speculative because of the complicated negative ion kinetics of flames.

Although the molecular parameters of OH^- are not known in the same detail as those of O_2^- and NO^-, the available experimental evidence[71,72] indicates that the potential energy curves of OH and OH^- differ only by a vertical displacement and thus that the vibrational spacings of the two are approximately equal. If this were the case the lowest resonance level would be the fifth vibrational level of OH^- lying ~0.18 eV above the ground vibrational state of OH. Assuming that the resonance width were small enough so that Herzenberg's[22] theory would apply, this high activation energy would imply that the room temperature attachment rate constant for OH would be much smaller than that for O_2.

4. Other Diatomics

The remaining diatomics important in the $O_2/N_2/H_2O/CO_2$ system, i.e., N_2, H_2 and CO, do not form stable negative ions. The halogen diatomic molecules do form stable negative ions; however, direct electron attachment to these species is unlikely since dissociative attachment (see section III) is an exothermic channel. The values listed in Table II for I_2 and Br_2 are deduced from Truby's[73-75] observations of dissociative attachment and should be considered strong upper bounds.

Christophorou et al.,[76] in a combined electron beam-drift tube study, observed an attachment process at near-zero electron energy for the molecules HCl, DCl, HBr, and DBr. The observed attachment cross section scaled with the square of the hydrogen halide pressure; however, the products were not identified. Stable negative ions of these species have not been observed; furthermore it was suggested in the above work that although it appears likely that HCl^- possesses a potential minimum, this minimum may lie above the ground state of HCl.

Davidow and Armstrong[77] found that a thermal attachment process involving HCl, i.e.

$$e + HCl + HCl \xrightarrow{k_{33}} \text{products} \qquad (33)$$

was required to explain their data on the yield of H_2, produced from the radiolysis of HCl in the presence of SF_6. From their observations they deduced a rate constant for process 33 of 2.6×10^{-30} cm^6 sec^{-1} at an HCl density of 1.6×10^{19} parts/cc. Johnson and Redpath,[78] in a similar study, found that the electron loss rate at thermal energies scaled as the cube of HCl density, over the density range of $2.5-10 \times 10^{19}$ parts/cc. They suggested the two-stage mechanism

$$e + HCl + HCl \rightleftarrows (HCl)_2^- * \qquad (34a)$$

$$(HCl)_2^- * + HCl \rightarrow \text{products} \qquad (34b)$$

to explain their results. The overall rate constant for process 34 was deduced to be 1.7×10^{-49} cm^9 sec^{-1}. At an HCl density of 1.6×10^{19} parts/cc, this would result in an effective three-body rate of 2.7×10^{-30} cm^6 sec^{-1}, in agreement with the result of Davidow and Armstrong.

It should be noted that process 34 would not be inconsistent with the observations of Christophorou et al.[76] since these latter measurements were made in mixtures of HCl highly diluted by N_2. In this case N_2 would be the stabilizing partner in reaction 34b, and the overall attachment process would appear to scale with the square of HCl density, as was observed in the drift tube measurements.

C. Triatomics

Attachment data are available for a number of triatomic molecules. Again a two-step model, such as reactions 10 and 11 is generally invoked to explain the various observations. In general the lifetimes of the excited states are expected to be long, $\gtrsim 10^{-10}$ sec, since there will typically be a number of low-lying states over which the excess energy can be distributed. A long lifetime implies the possibility of three-body saturation at pressures below an atmosphere, given efficient stabilizing collisions.

1. CO_2

CO_2^- has been observed to be formed in the gas phase via charge exchange reactions;[79] however, it does not appear to be created by a low-energy electron attachment process.[80] Ferguson et al.[81] have proposed a geometrical argument against the formation of CO_2^- by such a mechanism. They point out that nonhydrogen bearing triatomic molecules containing 16 valence electrons, such as CO_2 and N_2O, are linear in their ground electronic states while molecules with 17 valence electrons are bent in the ground state (Walsh rules).[82] Thus the formation of CO_2^- and N_2O^- would require a substantial deformation from the neutral configuration, and this could well produce a hindrance to electron attachment.

2. H_2O

H_2O^- has not been observed in the gas phase although evidence has been presented for its having a positive electron affinity.[83] Several experimenters[84-87] using either drift tubes or stationary afterglows have published lower bounds for attachment to H_2O, the lowest of these being listed in Table II. It has been suggested[87] that impurities were the cause of finite H_2O attachment rates deduced in earlier experiments.[84,85]

3. N_2O

There have been a number[64,88-92] of experimental studies of attachment to N_2O in recent years, and in all cases an apparent three-body attachment rate has been observed in contradiction to the expectations based on the geometrical argument presented by Ferguson et al.[81] This process has recently been studied by Parkes[64] via a drift tube with mass filter. He has demonstrated that at low pressures the apparent three-body attachment rate can be explained by a sequence of reactions initiated by dissociative attachment of N_2O, i.e.

$$e + N_2O \rightarrow O^- + N_2 \qquad (35)$$

followed by

$$O^- + N_2O \rightarrow NO^- + NO \qquad (36)$$

$$NO^- + N_2O \rightarrow NO + N_2O + e \qquad (37a)$$

$$\rightarrow NO_2^- + N_2 \qquad (37b)$$

$$NO^- + 2N_2O \rightarrow N_3O_2^- + N_2O \qquad (38)$$

$$O^- + 2N_2O \rightarrow N_2O_2^- + N_2O \qquad (39)$$

This reaction sequence provides reasonable agreement with the observations of Moruzzi and Dakin[90] as well as those of Parkes, and the various reaction rate constants deduced by Parkes have been confirmed in part in recent work by Warman et al.[92] and Marx et al.[65] Parkes has demonstrated

that the reaction sequence 35–39 should exhibit an overall third-order pressure dependence at low pressures but become second order above 30 Torr, whereas in the observations of both Phelps and Voshall[88] and Warman and Fessenden[89] the apparent attachment reaction was found to be third order up to pressures of 200 Torr. To explain this observation Parkes has postulated that an additional reaction must be included in the sequence 35–39, that being

$$e + N_2O + N_2O \rightarrow \text{a detaching ion} \quad (40)$$

with a rate constant of about 6×10^{-33} cm^6 sec^{-1}. The product of this reaction must either detach or produce a detachable ion in a subsequent reaction in order for sequence 35–40 to manifest a third-order pressure dependence over the full range of the observations, 1–200 Torr. Parkes has suggested that this ion is O^- created in a two-step process involving excited N_2O, i.e.

$$e + N_2O \leftrightarrow N_2O^- \quad (41)$$

$$N_2O^- + N_2O^* \rightarrow O^- + N_2 + N_2O \quad (42)$$

where the excited N_2O population arises from the Boltzmann distribution of states. Assuming this sequence Parkes has shown that the overall effective attachment rate remains third order with a rate constant of 6×10^{-33} cm^6 sec^{-1} over the pressure range 1–200 Torr. It can be shown that this remarkable result arises because $k_{35}/k_{40} = k_{37a}/k_{38}$. This is quite coincidental, and if a product ion other than O^- were proposed for reaction 40 it would be quite unlikely that the resultant effective attachment rate would have a similar behavior.

Two measurements[91,92] are available for the effective rate constant of attachment to N_2O with N_2 as the third body. These measurements differ by a factor of 6, and it is possible that neither is representative of the actual room-temperature attachment rate. The measurement of Chaney and Christophorou[91] was made at N_2/NO_2 ratios of 300 and greater where the reaction sequence 35–39 should be unimportant relative to direct attachment; however, the attachment rate was only measured at characteristic energies $\langle\epsilon\rangle > 0.18$ eV and the extrapolation to room temperature, $\langle\epsilon\rangle \sim 0.027$ eV, could be in error considering the complicated nature of the reaction. On the other hand, the measurement of Warman et al.[92] was made with thermal electrons, but the N_2/N_2O ratio in this work was only 7 and the effect of the reaction sequence 35–39 on the electron decay should be included in the analysis of the experimental data.

In any event the negative ion N_2O^- has not been observed in thermal energy electron attachment studies of N_2O. It would appear that the geometrical argument presented by Ferguson et al.[81] is valid and that the observed apparent three-body attachment rate constant in N_2O is due to a sequence of reactions.

4. O_3

Three-body attachment to O_3 has never been observed. The value listed in Table II is an upper bound deduced from the dissociative attachment measurements of Stelman et al.,[93] i.e.

$$e + O_3 \rightarrow O^- + O_2 \quad (43)$$

It should be pointed out that in this work the dissociative attachment reaction could not be distinguished from a saturated three-body attachment reaction

$$e + O_3\ (+M) \rightarrow O_3^-\ (+M). \quad (44)$$

However, the results of this experiment were in reasonable agreement with the low-pressure, mass-analyzed electron beam measurements of Chantry,[94] and on this basis it is assumed that the former process (eq 43) was indeed observed.

5. NO_2

A number of electron attachment measurements have been made in NO_2.[38,61,95-97] The attachment reaction has been found to be second order down to pressures as low as 0.2 Torr; however, the magnitude of the rate is found to vary with the nature of the third body. Mahan and Walker[95] suggested the following mechanism to account for these observations

$$e + NO_2 \underset{\tau_{45}^{-1}}{\overset{k_{45}}{\rightleftarrows}} NO_2^-* \quad (45)$$

$$NO_2^-* + M \xrightarrow{k_{46}} NO_2^- + M \quad (46)$$

$$NO_2^-* + M \xrightarrow{k_{47}} NO_2 + e + M \quad (47)$$

Making the steady-state approximation for NO_2^-* results in the equation

$$d(e)/dt = -\frac{k_{45}k_{46}(NO_2)(N)(e)}{\tau_{45}^{-1} + (k_{46} + k_{47})N} \quad (48)$$

When $\tau_{45}^{-1} < (k_{46} + k_{47})N$, the effective attachment rate is given by

$$k_{eff} = \frac{k_{45}k_{46}}{k_{46} + k_{47}} \quad (49)$$

and the reaction will scale as second order in pressure. The observed variation of the rate with nature of the third body was then attributed to variation of the ratio k_{46}/k_{47} for different M (which implies that this ratio is of order 1). Their measurements were made over the range of 3–70 Torr and, assuming that the rates for reaction 41 and 47 could be as large as the orbiting limit, would suggest that $\tau_{45} > 10^{-8}$ sec. Klots[50] has recently suggested that this mechanism is invalid. He pointed out that microscopic reversibility requires that $k_{-47}/k_{47} = \tau_{45}k_{45}$ and that therefore the reverse of reaction 47 must be included in the analysis. In this case eq 48 becomes

$$d(e)/dt = -\frac{k_{45}k_{46}(e)(NO_2)N(1 + \tau_{45}k_{47}N)}{\tau_{45}^{-1} + (k_{46} + k_{47})N} \quad (50)$$

It can be seen that when $\tau_{45}^{-1} < (k_{46} + k_{47})N$, a condition which in eq 48 implies a second-order dependence, eq 50 could require that the effective attachment rate be third order in contradiction with the observations.

Freeman[98] has pointed out that the situation is actually more complicated than indicated by Klots. He suggests that there is no reason that the excited state produced in the two-body reaction 45 be the same as that produced in the three-body reaction (the reverse of reaction 47). Indeed, in general, there may be a manifold of such states. While this point adds a constraint to Klots' criticism, it would appear that his main point, i.e., that the mechanism of Mahan and Walker is invalid, is still correct.

Van Lint et al.[96] have also studied attachment in NO_2. In this work the rate of electron decay in the afterglow of a pulse of ionization produced by high-energy electrons was followed via microwave techniques. The first measurements were made in pure NO_2, and it is not clear whether the observed attachment occurred before the electrons were thermalized. In the pressure range of 0.03–0.15 Torr the attachment was characterized by a third-order pressure dependence with a rate coefficient of 1.6×10^{-27} cm^6 sec^{-1}, but at higher pressures (0.15–0.9 Torr) the data appear to drop to second order with a rate coefficient of approximately 10^{-10} cm^3 sec^{-1}. While the scatter in the measurements, as well as the possibility of the electrons being suprathermal, leave the interpretation of these data open to question, the results would imply that the attachment reaction becomes saturated at about 0.15 Torr. Interpreting this within the framework of the simple mechanism (45)–(46) would imply $\tau_{48} \gtrsim 10^{-7}$ sec

and $k_{45}k_{46} \gtrsim 10^{-20}$ cm^6 sec^{-2}. Van Lint et al. also examined the attachment rate vs. pressure in several NO_2–M mixtures. They demonstrated that the electrons were thermalized before attachment only in their NO_2–He mixture. In this case they observed the attachment reaction to be second order at pressures of 10–100 Torr and third order at higher pressures. While the cause of this behavior is not known, one could conjecture that an impurity was present in the gas which attached via a third-order mechanism and thus became the dominant attacher at high pressures. The NO_2 attachment rate deduced from the 10–100 Torr data with He as a third body would be approximately 5×10^{-11} cm^3 sec^{-1} about 2.5 times larger than the rate observed by Mahan and Walker.[95] (It should be noted that Van Lint et al. interpreted the higher pressure data to be due to three-body attachment to NO_2 and the results at 10–100 Torr to be due to an impurity. In the light of the more recent measurements[38,61,95,97] it now appears that the reverse was true.)

It is clear that there is still much uncertainty in both the mechanism and rate for attachment to NO_2. For instance, the rate measurements of Hasted and Beg[97] (listed in Table II) are more than an order of magnitude lower than those of Mahan and Walker.[95] In the absence of other measurements with N_2 and Xe as collision partners the latter rates must be preferred solely on the basis that the rates measured in other experiments[38,61] with different third bodies all fall in the range 10^{-11}–10^{-10} cm^3 sec^{-1}. In any event all observations to date imply that the attachment reaction maintains second-order pressure dependence to pressures less than a torr at room temperature even for relatively inert collision partners.

6. SO_2

Bouby et al.[99] have recently presented measurements for attachment in SO_2 which display a similar behavior except that for some of the collision partners studied a third-order dependence was observed. No mechanism has been suggested to explain these results.

D. Larger Molecules

Electron attachment has been observed for a large number of complex molecules. The attachment reaction is typically second order since the lifetimes of the excited ions are expected to be long, $\geq 10^{-7}$ sec, and the attachment rates can be quite large, as high as 10^{-7} cm^3 sec^{-1}. A discussion of this data base is beyond the scope of this work, and the reader is referred to the recent text by Christophorou[2] and review by Christophorou and Blaunstein.[100]

III. Dissociative Attachment

Electron attachment may also occur via a dissociative process. The general form of this type of reaction is

$$e + AB \rightarrow A^- + B \qquad (51)$$

where A and B may be either atomic or molecular fragments. Such processes are generally considered to proceed in two steps, first an electronic transition of the system to the state AB^{-*}, i.e.

$$e + AB \rightarrow AB^{-*} \qquad (52)$$

which may then autodetach

$$AB^{-*} \rightarrow AB + e \qquad (53)$$

or dissociate

$$AB^{-*} \rightarrow A^- + B \qquad (54)$$

The basic difference between this process and that suggested by Herzenberg for direct attachment (section II) is that the resonance occurs about an autoionizing rather than a bound state of the system (see Figure 4a).

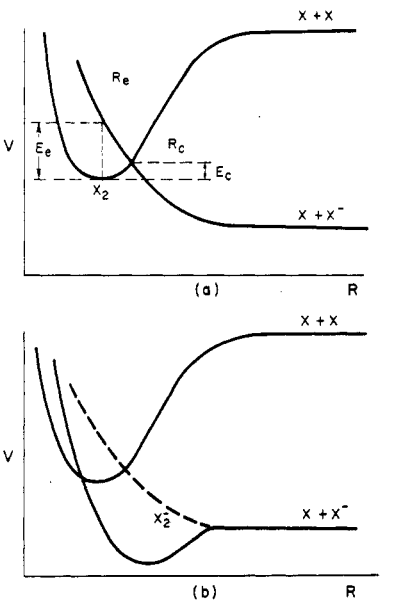

Figure 4. (a) Representative potential curves for exothermic dissociative attachment; (b) schematic potential curves for halogen molecules.

The process of dissociative attachment (DA) has been studied for a large number of molecular species and has attracted some theoretical effort.[101–108] Much of the data base has been reviewed in recent books by Christophorou[2] and Massey et al.,[109] although the main thrust in these works was toward reporting the cross-section measurements of endothermic reactions. The available data on exothermic or slightly endothermic reactions are reported in Table IV and discussed below.

A. Diatomics

O'Malley[101] has developed a theory for dissociative attachment of diatomic molecules which has been successfully applied to predicting both the electron and translational temperature dependence of the dissociative attachment cross section for the oxygen molecule.[103,110]

In his analysis O'Malley treated the process as a Feshbach[111] type resonance, behaving as shown by reactions 52–54, and used a projection-operator decomposition, based on the resonance state, and valid under the assumption of Born–Oppenheimer separation to develop the following general form of the cross section

$$\sigma_{v,r}(E) = \frac{4\pi^2 g}{k^2}\frac{\Gamma_{a,x}}{\Gamma_d}\left|\tilde{\chi}_v\left(R_e - \frac{i\Gamma_a}{\Gamma_d}\right)\right|^2 e^{-\rho} \qquad (55)$$

where E is the electron energy, the subscripts v and r refer to the vibrational and rotational states of the target molecule, k is the incident electron wave number, g is a statistical factor, $\Gamma_{a,x}$ and Γ_d are the partial widths for autoionization and dissociation respectively, Γ_a is the total autoionization width, and $\tilde{\chi}_v$ is the initial normalized wave function. These quantities are evaluated at R_e, the turning point of final state motion (see Figure 4a). The factor $e^{-\rho}$ is the survival probability defined approximately as

$$e^{-\rho} \simeq \exp\left(-\int_{R_e}^{R_c}\frac{\Gamma_a(R)\,dR}{\hbar v(r)}\right) \qquad (56)$$

where R_c is the crossing point between the potential curves for the resonant electronic state AB^{-*} and the initial state AB

TABLE IV. Dissociative Electron Attachment

$e + AB \rightarrow A^- + B$

Reaction	ΔHf_{298}, eV	T, °K	k, $cm^3 - sec^{-1}$	Ref.	Comments
1) $e + Br_2 \rightarrow Br^- + Br$	-1.43	298	$(8.2 \pm 0.8) \times 10^{-13}$	73b	
2) $e + Cl_2 \rightarrow Cl^- + Cl$	-1.17				See text
3) $e + DBr \rightarrow Br^- + D$	0.43	300	2.2×10^{-11}	76a, b	Deduced from cross-section data. Onset 0.11 eV.
4) $e + DI \rightarrow I^- + D$	0.02	300	9.6×10^{-8}	76a, b	Deduced from cross-section data.
5) $e + F_2 \rightarrow F^- + F$	-1.83	3600 - 6000	$2 - 0.2 \times 10^{-7}$	125e, i	See text and Fig. 5.
6) $e + HBr \rightarrow Br^- + H$	0.37	300	3×10^{-11}	76a, b	Deduced from cross-section data. Onset 0.11 eV. See text.
7) $e + HI \rightarrow I^- + H$	-0.033	300	2.0×10^{-7}	76a, b	Deduced from cross-section data.
8) $e + I_2 \rightarrow I^- + I$	-1.56	300	4.1×10^{-9}	131b	See text.
		250 - 520	$8.4 \times 10^{-9} \left(\frac{300}{T}\right) e\left(-1150/T\right)$	74a, 75a	Fit to data. See Fig. 7.
9) $e + N_2O \rightarrow O^- + N_2$	+0.20	400 - 1040	$\sim 10^{-11} - 10^{-7}$	139d	Deduced from cross-section data. See Fig. 8.
		278 - 355	$7.3 \times 10^{-8} e\left(-4800/T\right)^*$	92b	See Fig. 8.
		300	4×10^{-15}	64a, g	
		2800	2.5×10^{-10}	144	See text.
10) $e + O_3 \rightarrow O^- + O_2$	-0.43	300	$< 1 \times 10^{-11}$	146c	
		112 - 361	$2 - 3 \times 10^{-11}$	94d	Deduced from cross-section data. See Fig. 9.
		200 - 300	$8.9 \times 10^{-12} \left(\frac{T}{300}\right)^{3/2}$*	93a	See Fig. 9.
11) $e + HBO_2 \rightarrow BO_2^- + H$		1700 - 2450	$(3.2 \pm 1.6) \times 10^{-10} e\left(-10,600/T\right)$	149f	
12) $e + H_2O_2 \rightarrow O^- + H_2O$	-0.05				See text.
$\rightarrow OH^- + OH$	+0.37				

(see Figure 4a) and $v(r)$ is the classical velocity of the dissociating particles.

The cross section defined by (55) is fully determined if the potential curves of the initial and final states are known, including the width, Γ_a, of the latter. The attachment rate constant for temperature T is determined by first Boltzmann averaging the cross section over the rotational–vibrational distribution of the molecule and then integrating the product of this result and velocity over the electron distribution.

The problem here, of course, is that generally the shape of the relevant excited state potential curve is not known. (Conversely, however, the theory has been used in conjunction with cross-section data to deduce information about the excited state potentials of O_2^- [103] and I_2^-.[112]) Furthermore, as pointed out by Shipsey,[112] the arguments[104,105] which have been presented to justify the assumption of Born–Oppenheimer separation require that the vibrational spacing be small relative to the electron energy, which condition is not met for thermal processes. Because of this, while the phenomenology of the process is the same at thermal energies, expression 56 cannot be used to describe the survival probability.

Nonetheless, it is clear from the theoretical work that, although the rate constant for dissociative attachment will be characterized by an activation energy, $\sim E_c$, the general expression for the rate constant can be a complicated function of temperature and need not generally be expressible in terms of a simple Arrhenius expression. Furthermore, the rate constant will be strongly dependent on the vibrational rather than just the translational temperature since the process involves a curve crossing.

In the case of a diatomic molecule AB, dissociative attachment will be an exothermic process only if the electron affinity of A is greater than the bond strength of AB. None of the diatomics in the $O_2/N_2/H_2O/CO_2$ system come close to satisfying this stringent requirement. For instance, dissociative attachment of oxygen molecules is some 3.5 eV endothermic and has been shown[110] to have a rate constant of less than 10^{-16} cm^3 sec^{-1} at 2000°K.

As a group the halogen atoms have the highest atomic electron affinities, and molecules containing these atoms are most likely to have exothermic dissociative attachment channels. Indeed dissociative attachment of the halogen molecules Br_2, Cl_2, F_2, and I_2 is an exothermic process. Exothermicity, of course, does not guarantee that the attachment reaction will proceed with a meaningful rate constant at low temperatures as this will depend upon the energy at which the repulsive potential curve crosses that of the ground state. The halogen molecules are particularly interesting in that they also form stable molecular ions,[113] and it is possible that dissociative attachment could proceed via resonance excitation to the repulsive portion of the potential curve of the molecular ion rather than via resonance excitation to a purely repulsive electronic state. If DA proceeded via the aforementioned mechanism, the DA cross section would probably be small since the overlap between the repulsive portion of the potential curve of the ground-state molecular ion and the potential curve of the ground-state halogen molecule would be limited. This can be seen by reference to Figure 4b where schematic potential curves for a halogen molecule are shown.

Low-temperature dissociative attachment rate constant data are available for several of the halogen molecules. These measurements have typically been performed in stationary afterglows by monitoring electron density decay in the presence of halogen molecules via microwave techniques. Supplementing this work are other observations of the variation of the dissociative attachment cross section with electron energy. These latter measurements are usually performed either in a drift tube or with a narrow energy width electron beam.

It should be noted that there is a basic difference between the unfolded cross sections as determined by these latter two techniques. In the drift tube work the cross section at energy E is an average value over the electron energy distribution, which need not be Maxwellian, about the energy E. For the electron beam the cross section represents an average over the beam energy distribution.

Although the onset potential of a dissociative attachment reaction can be quite sensitive to the temperature, in principle some information about the activation energy of the process can be deduced from the cross-section data. In practice this is not the case since there is a wide disparity between the available cross-section data for the halogen molecules as is discussed below.

1. Br_2

The only measurement of the rate constant for dissociative attachment of Bromine is Truby's[75] value of 0.82×10^{-12} cm^3 sec^{-1} at 296°K determined in a stationary afterglow system. This corresponds to an average cross section, $\sigma = k/\bar{v}$, of 0.75×10^{-19} cm^2, where $\bar{v}$ is the average electron velocity. This process was first examined by Blewett[114] (electron beam with mass identification) who observed the peak cross section to occur at 2.8 eV and the cross section at ~0.5 eV to be approximately a factor of 10 lower. The uncertainty in the energy scale and the magnitude of the cross section were not defined in this work. These measurements were shortly followed by those of Bailey et al.[115] (drift tube) who observed the peak cross section to occur at 1.95 eV and the onset to occur at less than 0.7 eV. While the observed cross section fell off very rapidly for electron energies above 2.3 eV, the variation was very slow between there and 0.7 eV, being 1.46×10^{-18} cm^2 at the peak and 1.1×10^{-18} cm^2 at the onset. It should be mentioned that recently Razzack and Goodyear[116] have made a drift tube study of DA in bromine at higher energies. While the energy range of their work does not quite overlap with that of Bailey et al., their cross section at ~3.2 eV (using Bailey et al.'s relationship between electron energy and reduced field) is approximately a factor of 6 higher. Razzack and Goodyear suggest that the neglect of ionization in the analysis of Bailey et al. may be the major contribution to this discrepancy.

More recently Frost and McDowell[117] (electron impact with mass identification) have found the cross section to peak at 0.03 ± 0.03 eV and vanish at 0.72 ± 0.05 eV. Their result is not only in disagreement with the earlier observations of Blewett and of Bailey et al., but also it is doubtful that their observation could be consistent with the thermal cross section observed by Truby. Christophorou[118] has demonstrated that the data base for dissociative attachment cross sections manifests an inverse relationship between peak cross section and the energy at which the peak cross section occurs. Indeed molecules which have peak cross sections near zero electron energy typically have cross sections greater than 10^{-15} cm^2. Based on the available data and the magnitude of Truby's rate constant, it would appear that dissociative attachment of Br_2 does involve an activation energy which is probably $\lesssim 0.3$ eV (this upper bound being based upon the magnitude of Truby's room-temperature measurement).

2. Cl_2

The thermal rate constant for dissociative attachment of chlorine has not been measured. Bradbury[119] (drift tube) observed the attachment probability to increase with increasing electron energy at low reduced field. His work was shortly followed by Bailey and Healey[120] (drift tube) who found the cross section to be fairly constant at 10^{-18} cm^2 for electron energies between 0.31 and 1.43 eV and to fall off rapidly at higher energies. This is equivalent to a rate constant ($k = \sigma\bar{v}$) of 3.3×10^{-11} cm^3 sec^{-1} at 0.31 eV. Recently, Bozin and Goodyear[121] (drift tube) examined electron attachment to chlorine at higher energies and found that where their data overlapped those of Bailey and Healey, at approximately 3.4 eV (using the electron energy vs. reduced field data of Bailey and Healey), their measured cross section was approximately a factor of 9 higher. Again it was suggested that the discrepancy may be due to the neglect of ionization effects in the earlier work.

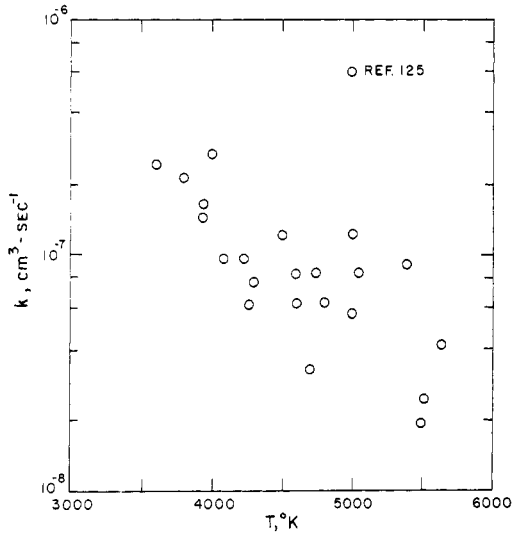

Figure 5. The rate constant for the reaction $e + F_2 \rightarrow F + F^-$ vs. gas temperature.

Thorburn[122] (electron impact with mass identification) observed that the onset potential for dissociative attachment in Cl_2 was less than 2 eV, the lowest energy employed. This work was shortly followed by that of Frost and McDowell[117] where an onset potential of 1.6 eV and peak cross section at 2.4 eV was observed. As in the case of Br_2, these measurements of Frost and McDowell are in disagreement with the earlier observations. Furthermore Dunkin et al[123] (flowing afterglow) have recently observed dissociative attachment of Cl_2 to proceed with thermal energy electrons. This observation would seem to preclude an onset potential as high as 1.6 eV.

3. F_2

There had been no measurements of the rate constant for dissociative attachment of fluorine until quite recently. The earlier observations were those of Burns[124] (electron impact with mass identification) who reported DA of F_2 with thermal electrons and Thorburn[122] who reported that the onset potential for this process occurred at electron energies less than 2 eV, the lowest energy available to him. Recently Mandl,[125] in a shock tube experiment (see section II), has measured the rate constant for the reverse reaction, i.e.

$$F^- + F \rightarrow F_2 + e \qquad (57)$$

between the temperature range of 3600 and 5600°K. Detailed balancing has been applied to Mandl's data in order to determine the DA rate constant, and these results are shown in Figure 5. These results seem to imply a very strong temperature dependence, of order T^{-4}, for the rate constant. This may not be the case, however, both because shock tube rate constant data typically are uncertain to within a factor of 2, and, perhaps more importantly, the equilibrium constant for reaction 57 varies by a factor of 35 over this limited tempera-

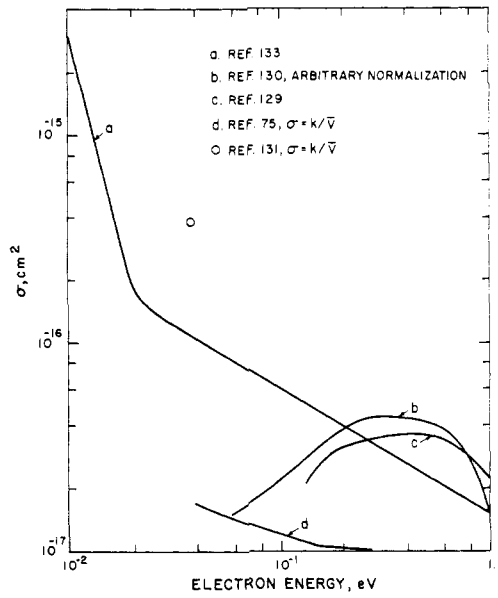

Figure 6. Measurements of the cross section for the reaction $e + I_2 \rightarrow I + I^-$ plotted vs. electron energy.

ture range and thus the effect of any misassignment in shock temperature could be greatly magnified.

DA of F_2 is not of general interest at the elevated temperatures of Mandl's experiment because of the low dissociation energy of F_2. The important conclusion that can be drawn from Mandl's data is that since the DA rate constant is of order 10^{-7} cm^3 sec^{-1} at 3600°K, one would expect the activation energy for the process to be small, less than a few tenths of an electron volt. This result is in agreement with Burns' observations.[124]

It should be mentioned here that, in general, dissociative attachment rate constants determined by the detailed balancing or associative detachment rate constants may not be reliable. The reason for this is that the products of an associative detachment reaction may be created in an excited state, in which case detailed balancing using *equilibrium* partition functions could be invalid. In the case of Mandl's data on F_2 the translational temperatures are so high that such nonequilibrium effects should be relatively unimportant.

4. I_2

Off all the halogen molecules, iodine has been studied in the most detail; however, once again there are wide discrepancies between the various measurements. In early observations both Mohler[126] (electron beam with mass identification) and Hogness and Harkness[127] (electron beam with mass identification) observed dissociative attachment of I_2 with low-energy electrons. The first quantitative measurement of the cross section was made by Healey[128] (drift tube) who observed the onset to occur at electron energies of less than 1 eV and the peak cross section to occur at 2.4 eV. The cross section was found to vary from 3.2×10^{-18} to 1×10^{-17} cm^2 over that energy range. Shortly thereafter Buchdahl[129] (electron beam) observed onset to occur at <0.13 eV with peak cross section at ~0.4 eV. These data, out to 1.0 eV, are shown in Figure 6. Buchdahl also observed subsidiary peaks at higher energies. Frost and McDowell[117,130] performed a similar investigation and found onset to occur at 0.03 ± 0.03 eV and peak cross section to occur at 0.34 ± 0.07 eV. While the magnitude of the cross section was not determined in this investigation, the shape of the resulting ion current curve is very similar to Buchdahl's observations as can be seen by reference to Figure 6. No subsidiary peaks at higher electron energy were observed in this experiment; however, it was found that such peaks could be caused by instrumentation effects, and this may account for Buchdahl's earlier observations.

The thermal rate constant for DA of I_2 was measured by Biondi[131] by following the rate of electron decay in I_2–He mixtures via microwave techniques in a stationary afterglow. The measured rate constant was 4.2×10^{-9} cm^3 sec^{-1} or an average cross section of 3.9×10^{-16} cm^2. Simultaneously Fox[132] (electron beam with mass identification) observed the cross section variation at low electron energies and found it to peak at essentially zero energy. In this work the electron energy distribution of the electron beam could be deduced and the actual cross-section variation was obtained by a deconvolution of the measured cross section.[133] This resulting cross section was found to be very strongly peaked near zero electron energy as is shown in Figure 6. The magnitude of the cross section was determined by use of Biondi's room-temperature measurement of the rate constant. Both Biondi's and Fox's experiments suffered from contamination by HI. This can be a serious problem since it has recently been shown[76] that dissociative attachment of HI has a very large cross-section peaking at essentially zero electron energy. Mass spectrometry was available in Fox's experiment, and it was demonstrated that although HI was not initially present in his system its concentration increased slowly with time upon the addition of I_2. Fox pointed out that in his experiment the shape of the I^- current vs. electron energy did not change with increasing HI concentration, although it did increase in magnitude, and therefore he concluded that the energy dependence of the DA cross sections for I_2 and HI were quite similar.

Recently Truby,[73,74] employing a stationary afterglow device, has measured the DA rate constant for I_2 over a limited range of translational temperature and electron energy. In this work the electron energy was varied by microwave heating. Truby's measurements of "average" cross section are shown in Figure 6 and vary only by some 50% between electron energies of 0.04 to 0.27 eV. The thermal rate constant deduced in this work is some factor of 20 below that observed by Biondi. One basic difference between the two experiments is that Truby employed a single ionization pulse technique whereas Biondi's experiment utilized a repetitive ionization pulse. Truby[73] has demonstrated that, at an iodine pressure of 10^{-3} Torr, the application of repetitive pulses resulted in a factor of 6 increase in the electron decay rate over that for a single pulse. Given this observation, as well as the possible impurity effects in Biondi's experiment, Truby's measurement must be preferred.[134] Therefore, the absolute value of Fox's[132] cross section, which was originally scaled from Biondi's results, should be decreased by a factor of 23 in order to bring it into agreement with Truby's work.

The variation of Truby's rate constant with translational temperature is shown in Figure 7. The solid curve is a fit to the data and involves an activation energy of ~0.1 eV. There is no theoretical justification for the functional form of the rate constant shown, and it should not be liberally extrapolated to other temperature ranges. Shipsey[112] has analyzed Truby's data in terms of O'Malley's[10] theory and finds that a best fit results for a crossing energy, E_c, of 0.066 ± 0.007 eV above the ground-state energy of I_2. This interpretation of Truby's results is, of course, inconsistent with Fox's observations.

It is clear from the above discussion that there is still much uncertainty concerning dissociative attachment of the halogen molecules. Experimental work would be valuable in this area not only because the halogen molecules represent a fundamental system amenable to theoretical analysis but also because halogen dissociative attachment cross-section data

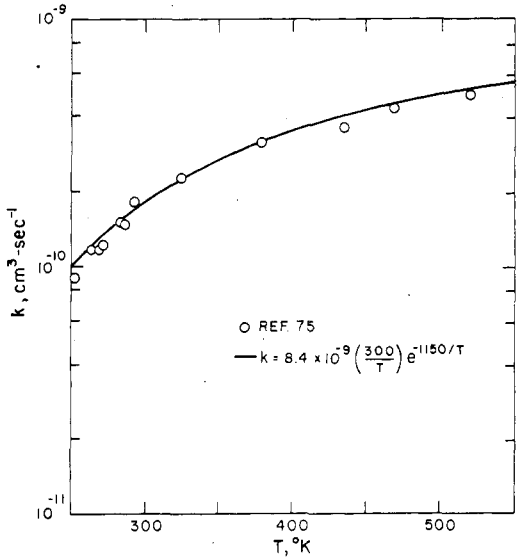

Figure 7. The rate constant for the reaction $e + I_2 \rightarrow I + I^-$ vs. gas temperature. The solid curve is a curve fit of the experimental data.

could be of immediate use in the analysis of electrical discharge laser systems presently under study.[135]

A last point with reference to section II. The halogen molecular negative ions have also been observed in several of the experiments discussed above,[114,116,127,129] and in at least one case[116] it has been suggested that these were created in a three-body attachment process. Blewett,[114] in the case of Br_2, and Buchdahl,[129] in the case of I_2, have shown that approximately half the energy released in the dissociative attachment process is converted to translational energy of the negative ion. (Assuming no excited states are created, this is expected based on momentum considerations.) What this implies is that, with the exception of Cl_2, dissociative attachment, even if by thermal electrons, would create negative halogen ions with sufficient translational energy to allow the endoergic charge-transfer reaction, i.e.

$$X^- + X_2 \rightarrow X_2^- + X \qquad (58)$$

to occur. The extent of X_2^- production in a given experiment would, of course, depend on the cross section for process 58 as well as the density of the buffer gas, as this gas would act as a thermalizing agent for the atomic ions. It would appear that process 58 would be a more reasonable production source for the observed halogen molecular ions than direct attachment.

To the author's knowledge the only other diatomic molecules with exothermic (or slightly endothermic) dissociative attachment channels which have been studied are the hydrogen halides HI and HBr and their deuterated analogs. The absolute DA attachment cross section vs. electron energy, corrected for the experimental electron energy distribution, were measured by Christophorou et al.[76] using a combination of drift tube and electron beam techniques. The relevant cross sections were quite large and in the case of HI/DI peaked at zero electron energy. The thermal rate constants for these processes are listed in Table IV and were obtained by integrating the observed cross section multiplied by the electron velocity over a Maxwellian velocity distribution at $T = 300°K$. In the case of HBr/DBr the published cross sections[76] were adjusted so as to fall to zero at 0.11 eV.[136] (It should be pointed out that this observed onset is well below the reaction endothermicity of 0.37 eV. The cause of this is not understood and the listed rate constant should be used with caution.)

B. Triatomic and Larger Molecules

Several of the larger molecules in the $O_2/N_2/H_2O/CO_2$ system have exothermic or slightly endothermic dissociative attachment channels. The most studied of these is N_2O, involving the reaction

$$e + N_2O \xrightarrow{k} O^- + N_2 \qquad (59)$$

which is endothermic by 0.21 eV.

The impetus for detailed study of this process involved early observations that the onset for this reaction occurred at electron energies of 0.0–0.10 eV.[137,138] Not only was this low onset disallowed energetically, but Ferguson et al.[81] have pointed out that the production of N_2O^- ($[N_2O^-]^*$ in the case of reaction 59) should require a substantial deformation of the geometry of neutral N_2O. If this were the case an activation energy larger than the endothermicity would be expected. Lastly the reverse reaction, associative detachment, could be an important aeronomic process, and its rate constant might be related to that of DA via detailed balancing (see, however, discussion on F_2).

There is also an apparent three-body attachment process involving N_2O (see section II), and early observations of the DA rate constant were obtained by plotting the effective two-body attachment rate constant vs. pressure and setting the zero pressure intercept of this line equal to the DA rate constant.

Phelps and Voshall[88] (drift tube) and Warman and Fessenden[89] (stationary afterglow) both found the thermal DA rate constant to be less than 3×10^{-15} cm^3 sec^{-1} using this technique. More recently[64] it has been demonstrated that these results are invalid since in actuality a sequence of reactions occur simultaneously, i.e., eq 60, which are rapid and have the effect of detaching electrons and thus reducing the apparent overall attachment rate.

$$\begin{aligned} e + N_2O &\rightarrow O^- + N_2 \\ O^- + N_2O &\rightarrow NO^- + NO \\ NO^- + M &\rightarrow NO + e + M \end{aligned} \qquad (60)$$

Chaney and Christophorou,[91] using complementary drift tube and electron beam techniques, reexamined the variation of cross section vs. electron energy for process 59 and found that the cross section below 1.5 eV was quite sensitive to gas temperature. This result was quantified in a definitive electron beam study performed by Chantry[139] in which the gas temperature was varied between 160 and 1040°K. In this work it was found that the low-energy cross section was very sensitive to temperature and that with increasing temperature a peak in the cross section occurred very close to zero electron energy. The DA rate constants, as deduced by Warman et al.[92] from Chantry's data, are shown in Figure 8. These results imply that vibrational excitation of N_2O can strongly enhance the DA cross section, and the theoretical implications of this are discussed in some detail by Chantry[139] and Bardsley.[140]

Wenthworth et al.,[141] employing the thermal electron capture technique, examined dissociative attachment of N_2O over the temperature range of 207–488°K and found the rate constant to be characterized by an activation energy of 0.45 ± 0.02 eV, which they demonstrated to be consistent with Chantry's observations.

Recently Warman et al.[92] studied process 59 in a stationary afterglow over the temperature range of 278 to 355°K using the zero pressure intercept technique described above to determine the DA rate constant. Reaction sequence 60 was circumvented in this experiment by using saturated hydrocarbons (RH) as the diluent gas. These molecules, as a class, allow a rapid reaction of the form

$$O^- + RH \rightarrow OH^- + R \quad (61)$$

which effectively prevents the formation of NO^- and thus its subsequent detachment. Their resulting rate constant data are shown in Figure 8 and are best fit by the relation

$$k = 7.3 \times 10^{-8} e^{-4800/T} \text{ cm}^3 \text{ sec}^{-1} \quad (62)$$

corresponding to an activation energy of 0.42 ± 0.04 eV. Warman et al. point out that, although this activation energy is in good agreement with that determined by Wentworth et al.,[141] the latter measurements were made in the presence of a large excess of argon gas and there is the possibility that those measurements were effected by the three-body process. It should be noted that the extrapolation of relationship 62 to higher temperatures falls an order of magnitude below Chantry's[139] observations.

Parkes[64] has measured the thermal rate constant for process 59 using drift tube techniques and accounting for the reaction sequence 60 in his analysis. His result is in good agreement with that of Warman et al.

There is an additional high-temperature measurement of the DA rate constant which has been made by Mullen et al.[142-144] via mass spectrometric observations of negative ions in an expanding jet of a high temperature plasma. Unfortunately the data interpretation on this experiment appears complicated, and it is difficult to evaluate the validity of the published rate constants.

Initially, a rate constant of 1.8×10^{-10} cm^3 sec^{-1} was reported,[142] deduced at conditions corresponding to a gas temperature of 3000°K and electron temperature of 5300°K. In the following year analysis of additional data resulted in rate constants of 3×10^{-9} cm^3 sec^{-1} at 2500°K and 8×10^{-9} at 2900°K.[143] These values were in reasonable agreement with an Arrhenius extrapolation of the data of Warman et al.[92] Most recently, however, the experimental results were found to be affected by the geometry of the experimental system.[144] The system was modified and an analysis of the most recent data resulted in a rate constant of 1.3×10^{-10} cm^3 sec^{-1} at a temperature of 2800°K. This rate constant may well be a lower bound inasmuch as the effects of collisional detachment were not included in the data analysis.

The available rate constant data for dissociative attachment of N_2O are summarized in Figure 8. At low temperatures the data of Warman et al.[92] appear quite reasonable considering the agreement with Parkes'[64] room-temperature result. However, at higher temperatures the discrepancy between the extrapolation of the results of Warman et al. and Chantry's[139] data remains to be resolved.

Ozone has two dissociative attachment channels, the first of these

$$e + O_3 \rightarrow O^- + O_2 \quad (63)$$

being exothermic by 0.43 eV and the second

$$e + O_3 \rightarrow O_2^- + O \quad (64)$$

being endothermic.

The thermal rate constant for reaction 63 was first reported by Fehsenfeld et al.[145] to be 4×10^{-11} cm^3 sec^{-1}; however, shortly thereafter Fehsenfeld and Ferguson[146] reported that they had found that the electrons in the former experiment had not thermalized and that the rate constant was quite sensitive to electron temperature. The thermal rate constant was reported to be less than 10^{-11} cm^3 sec^{-1} in this latter paper.

Chantry[94] (electron beam with mass analysis) studied dissociative attachment of O_3 and found that at low electron energies the cross section for *both* dissociative attachment channels was independent of gas temperature over the temperature range of 112–361°K. Chantry's cross-section data

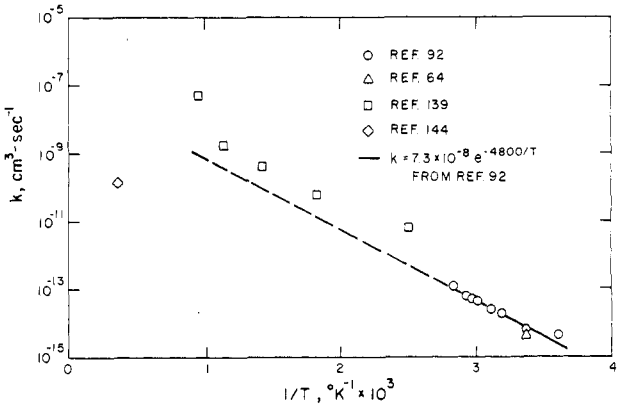

Figure 8. Measurements of the rate constant for the reaction e + $N_2O \rightarrow O^- + N_2$ plotted vs. the reciprocal of gas temperature.

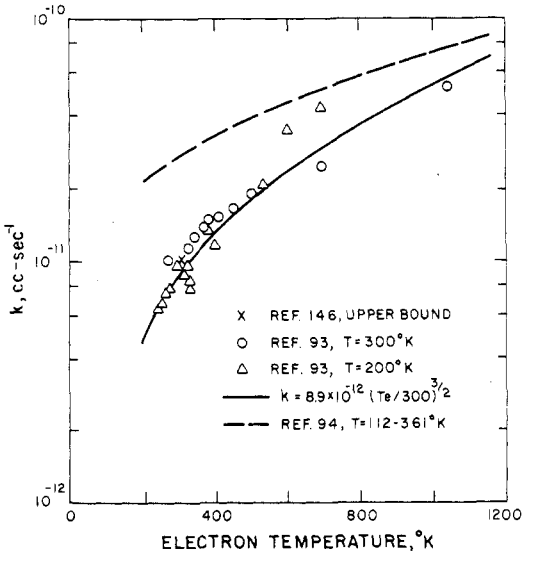

Figure 9. Measurements of the rate constant for the reaction e + $O_3 \rightarrow O^- + O_2$ plotted vs. electron temperature.

for process 63 has been converted into rate constants by Stelman et al.,[93] who accounted for the width of the electron beam in their conversion. The resulting rate constant vs. electron temperature is shown in Figure 9. The rate constant for gas temperatures between 112 and 361°K is the same as that for the respective range of electron temperatures.

Stelman et al.[93] have measured the rate constant for process 63 vs. characteristic electron energy (kT_e if the electron energy distribution is assumed to be Maxwellian) and found the distributions to be identical at temperatures of 200 and 300°K. These results are also plotted in Figure 9 under the assumption that the drift tube energy distribution was indeed Maxwellian. The agreement between these data and Chantry's is reasonable although the two sets of data begin to diverge at the lowest temperatures. The data of Stelman et al. are to be preferred both because of the agreement between their measurement and Fehsenfeld and Ferguson's[146] upper bound at room temperature, and also because of the electron beam width of ~0.1 eV in Chantry's experiment.

The solid line on Figure 9 is Stelman et al.'s fit to their data and is given by

$$k = 9 \times 10^{-12} (T_e/300)^{3/2} \text{ cm}^3 \text{ sec}^{-1} \quad (65)$$

The available measurements demonstrate that, in the range of 100–400°K, T_e may be replaced by the translational temperature T in expression 65.

The last of the air/H_2O/CO_2 molecules to be considered is H_2O_2 which has two DA channels.

$$e + H_2O_2 \rightarrow O^- + H_2O \qquad \Delta H_{f298} = -0.05 \text{ eV} \qquad (66)$$

$$\rightarrow OH^- + OH \qquad \Delta H_{f298} = +0.38 \text{ eV} \qquad (67)$$

Processes 66 and 67 have been examined by Curran[147] (electron beam with mass identification) who found that the onset potentials for both O^- and OH^- production occurred very close to zero electron energy, with the OH^- current being an order of magnitude higher than that of O^- even though the former is produced in an endothermic reaction. The beam width in this experiment was 0.3 eV.

Dissociative attachment has been studied for a number of larger molecules (five or more atoms) particularly that class containing halogen atoms. Some of these have been shown to have quite large cross sections at thermal electron energies. For example, the reaction

$$e + CCl_4 \rightarrow CCl_3 + Cl^- \qquad (68)$$

has been shown[118] to have a large low-energy cross section similar to that for HI. A discussion of the DA data for such molecules is beyond the scope of this work. The reader is referred to the Christophorou's text[2] and to the recent work by Spence and Schulz.[148]

The rate constant for DA of HBO_2[149] has been included in Table IV even though this reaction is endothermic by close to 1 eV. This reaction has been included because to the author's knowledge it is the only example of an endothermic dissociative attachment reaction whose rate constant has been measured. As mentioned earlier such rate constants should not be estimated by detailed balancing of the reverse associative detachment rate (which is typically only known at room temperature).

Acknowledgments. The author wishes to thank Drs. R. E. Center, A. V. Phelps, and R. L. Taylor for many useful discussions and comments on the subject matter of this report. Drs. L. G. Christophorou, A. Mandl, W. Miller, and V. H. Shui were kind enough to supply their data to the author prior to publication. This work was supported in part by the Advanced Research Projects Agency and Army Ballistic Missile Defense Agency under Contract DAHC60-69-0013.

IV. Addendum

There have been several studies of electron attachment reactions since this review was first prepared. These are discussed briefly below.

A. Three-Body Electron Attachment

Three-body attachment to SO_2 has recently been examined by Guillerez and Bouby[150] and by Rademacher et al.[151] in drift experiments. The former study was performed over the pressure range of 20–160 Torr and was in agreement with the earlier work of Bouby et al.[99] with the exception of measurements performed with C_2H_4 as the carrier gas. The basic conclusion was that electron attachment to SO_2 with N_2 as the third body appeared to be a bimolecular reaction for pressures between 20 and 160 Torr with a rate constant of $\sim 3.6 \times 10^{-12}$ cc/sec. On the other hand, with C_2H_4 as the third body, the attachment reaction appeared termolecular over the same pressure range with an apparent third-body rate constant of $\sim 6.4 \times 10^{-30}$ cm^6/sec.

Rademacher et al.[151] examined electron attachment to SO_2 with N_2 and C_2H_4 carrier gases over the pressure range of 200–2500 Torr and found that in both gases the attachment reaction was initially termolecular in the lower pressure range, becoming bimolecular at higher pressures. Their results extrapolated uniformly into the low-pressure data of Guillerez and Bouby.[150]

Rademacher et al. have developed a kinetic mechanism to explain these observations. This scheme involves a set of three reactions: (1) the two-body attachment/autoionization reaction 10; (2) collisional stabilization, reaction 11; and (3) radiative stabilization. They suggest that at low pressures radiative stabilization will dominate collisional stabilization, and thus the attachment rate will appaar bimolecular. With increasing pressure the reaction will become termolecular and subsequently bimolecular as discussed previously for the reaction sequence 10–11.

From an analysis of the data in terms of this reaction sequence it was found that the initial attachment reaction 10 proceeded with a rate constant of $\sim 8 \times 10^{-11}$ cc/sec, the ratio of autoionization to radiative stabilization lifetimes was ~ 0.03, the product of the collisional stabilization rate constant times autoionization lifetime was 2.0×10^{-21} cc for N_2 and 60 times larger for C_2H_4, and the autoionization lifetime was $> 1.8 \times 10^{-10}$ sec.

B. Dissociative Attachment

(1) Br_2. Sides and Tiernan[152] have recently examined DA of Br_2 in a flowing afterglow device and reported that $k_a \gg 10^{-12}$ cc/sec in contradiction with Truby's[73] earlier measurement.

(2) F_2. Sides and Tiernan[152] also have examined DA of F_2 and report an attachment rate constant of $(7.5 \pm 1.9) \times 10^{-9}$ cc/sec for an electron temperature of 500°K. This result would be consistent with an extrapolation of Mandl's shock tube results.[125]

(3) HCl. Burdett and Hayhurst[153] have examined DA of HCl, producing Cl^-, in a flame experiment at temperatures between 1800 and 2659°K. In this work detailed balancing was applied to a measurement of the reverse (associate detachment) rate constant resulting in $k_a = 2 \times 10^{-5} T^{-1/2} \exp(-9500 \cdot T)$ cc/sec.

(4) HNO_3. Fehsenfeld and Howard[154] have observed room-temperature dissociative attachment of HNO_3, producing NO_2^-, in a flowing afterglow device. The rate constant for this process is $k_a = (5^{+5}_{-3}) \times 10^{-8}$ cc/sec.

V. References

(1) E. W. McDaniel, V. Cermak, A. Dalgarno, E. E. Ferguson, and L. Friedman, "Ion-Molecule Reactions," Wiley-Interscience, New York, N.Y., 1970.
(2) L. G. Christophorou, "Atomic and Molecular Radiation Physics," Wiley-Interscience, New York, N.Y., 1971.
(3) P. Langevin, *Ann. Chim. Phys.*, **5**, 245 (1905).
(4) G. Gioumousis and D. P. Stevenson, *J. Chem. Phys.*, **29**, 294 (1958).
(5) M. Henchman in "Ion-Molecule Reactions," J. L. Franklin, Ed., Plenum Press, New York, N.Y., 1972, pp 101–260.
(6) M. I. Chibisov, *Sov. Phys.-JETP*, **22**, 593 (1966).
(7) R. Z. Vitlina and A. V. Chaplik, *Sov. Phys.-JETP*, **25**, 634 (1967).
(8) V. H. Shui and J. C. Keck, *J. Chem. Phys.*, **59**, 5242 (1973).
(9) R. E. Good, Mithras Report NASA CR-516, 1966, unpublished.
(10) A. P. Modica, *J. Phys. Chem.*, **71**, 3463 (1967).
(11) J. Debiesse, A. Von Engel, and S. Klein, *C. R. Acad. Sci., Ser. B*, **262**, 1121 (1966).
(12) E. J. Robinson and S. Geltman, *Phys. Rev.*, **153**, 4 (1967).
(13) J. J. Ewing, R. Milstein, and R. S. Berry, 7th Shock Tube Symposium, Toronto, Canada, 1969.
(14) A. Mandl, B. Kivel, and E. W. Evans, *J. Chem. Phys.*, **53**, 2363 (1970).
(15) A. Mandl, *J. Chem. Phys.*, **54**, 4129 (1971).
(16) A. Mandl, *J. Chem. Phys.*, **55**, 2922 (1971).
(17) A. Mandl, *J. Chem. Phys.*, **57**, 5617 (1972).
(18) A. Mandl, unpublished results.
(19) K. Luther, J. Troe, and H. G. Wagner, *Ber. Bunsenges. Phys. Chem.*, **76**, 53 (1972).
(20) L. Frommhold in "Atomic Collision Processes," M. R. C. McDowell, Ed., North Holland Publishing Co., Amsterdam, 1964, p 556; L. Frommhold, *Fortschr. Phys.*, **12**, 597 (1964).
(21) F. Bloch and N. E. Bradbury, *Phys. Rev.*, **48**, 689 (1935).
(22) A. Herzenberg, *J. Chem. Phys.*, **51**, 4942 (1969).
(23) C. J. Chapman and A. Herzenberg, Abstracts of the VIIth International Conference on the Physics of Electronic and Atomic Collisions, L. M. Branscomb et al., Ed., North-Holland Publishing Co., Amsterdam, 1971, p 1166.
(24) G. Breit and E. Wigner, *Phys. Rev.*, **49**, 519 (1936); see also J. M. Blatt and V. F. Weisskopf, "Theoretical Nuclear Physics," Wiley, New York, N.Y., 1952, p 392.
(25) R. D. Hake and A. V. Phelps, *Phys. Rev.*, **158**, 70 (1967).

(26) F. Koike and T. Watanabe, *J. Phys. Soc. Jpn.*, **34,** 1022 (1973).
(27) (a) D. Spence and G. J. Schulz, *Phys. Rev. A*, **5,** 724 (1972); (b) C. J. Chapman and A. Herzenberg, unpublished results as given in ref 27a.
(28) J. L. Pack and A. V. Phelps, *J. Chem. Phys.*, **44,** 1870 (1966).
(29) R. Grunberg, *Z. Naturforsch. A*, **24,** 1039 (1969).
(30) V. A. J. Van Lint, E. G. Wilkner, and D. L. Trueblood, *Bull. Am. Phys. Soc.*, **5,** 122 (1960).
(31) J. J. Lennon and M. J. Mulcahy, *Proc. Phys. Soc.*, **78,** 1543 (1961).
(32) L. M. Channin, A. V. Phelps, and M. A. Biondi, *Phys. Rev.*, **128,** 219 (1962).
(33) B. G. Young, A. W. Johnson, and J. A. Carruthers, *Can. J. Phys.*, **41,** 625 (1963).
(34) J. L. Pack and A. V. Phelps, *J. Chem. Phys.*, **45,** 4316 (1966).
(35) J. A. Stockdale, L. G. Christophorou, and G. S. Hurst, *J. Chem. Phys.*, **47,** 3267 (1967).
(36) A. V. Phelps, *Can. J. Chem.*, **47,** 1783 (1969).
(37) M. N. Hirsh, P. H. Eisner, and J. A. Slevin, *Phys. Rev.*, **178,** 175 (1969).
(38) L. Bouby, F. Fiquet-Fayard, and Y. Le Coat, *Int. J. Mass Spectrom. Ion Phys.*, **3,** 439 (1970).
(39) J. W. Warman, K. M. Bansal, and R. W. Fessenden, *Chem. Phys. Lett.*, **12,** 211 (1971).
(40) V. A. J. Van Lint, J. F. Colwell, and D. A. Vroom, Air Force Weapons Lab., Report AFWL-TR-70-115, 1971 (unpublished).
(41) D. A. Parkes and T. M. Sugden, *J. Chem. Soc., Farad. Trans. 1*, **68,** 600 (1972).
(42) F. K. Truby, *Phys. Rev. A*, **6,** 671 (1972).
(43) D. L. McCorkle, L. G. Christophorou, and V. E. Anderson, *J. Phys. B*, **5,** 1211 (1972).
(44) L. G. Christophorou, *J. Phys. Chem.*, **76,** 3730 (1972).
(45) R. F. Goans and L. G. Christophorou, *J. Chem. Phys.*, **60,** 1036 (1974).
(46) R. Freeman, E. Chen, and W. E. Wentworth, presented at 163rd National Meeting of the American Chemical Society, Boston, Mass., April 10–14, 1972 (unpublished).
(47) G. S. Hurst and T. E. Bortner, *Phys. Rev.*, **114,** 116 (1959).
(48) J. A. D. Stockdale, R. N. Compton, G. S. Hurst, and P. W. Reinhardt, *J. Chem. Phys.*, **50,** 2176 (1969).
(49) L. G. Christophorou, D. L. McCorkle, and V. E. Anderson, *J. Phys. B*, **4,** 1163 (1971).
(50) C. E. Klots, *J. Chem. Phys.*, **53,** 1616 (1970).
(51) J. E. Land and W. Raith, presented at Third International Conference on Atomic Physics, Boulder, Col., Aug 7–11, 1972 (unpublished).
(52) D. Spence and G. J. Schulz, *Phys. Rev. A*, **2,** 1802 (1970).
(53) F. Linder and H. Schmidt, *Z. Naturforsch. A*, **26,** 1617 (1971).
(54) R. J. Cellotta, R. A. Bennett, M. W. Siegel, and J. Levine, *Phys. Rev. A*, **6,** 631 (1972).
(55) C. A. Long and G. E. Ewing, *Chem. Phys. Lett.*, **9,** 225 (1971).
(56) C. A. Long and G. E. Ewing, *J. Chem. Phys.*, **58,** 4824 (1973).
(57) R. C. Gunton and E. C. Y. Inn, *J. Chem. Phys.*, **35,** 1896 (1961).
(58) R. C. Gunton and T. M. Shaw, *Phys. Rev. A*, **140,** 748 (1965).
(59) C. S. Weller and M. A. Biondi, *Phys. Rev.*, **172,** 198 (1968).
(60) M. H. Mentzoni and J. Donohue, *Can. J. Phys.*, **45,** 1565 (1967).
(61) L. J. Puckett, M. D. Kregel, and M. W. Teague, *Phys. Rev.*, **4,** 1659 (1971).
(62) M. McFarland, D. B. Dunkin, F. C. Fehsenfeld, A. L. Schmeltekopf, and E. E. Ferguson, *J. Chem. Phys.*, **56,** 2358 (1972).
(63) D. A. Parkes and T. M. Sugden, *J. Chem. Soc., Farad. Trans. 2*, **68,** 600 (1972).
(64) D. A. Parkes, *J. Chem. Soc., Farad. Trans. 1*, **11,** 2121 (1972).
(65) R. Marx, G. Mauclaire, F. C. Fehsenfeld, D. B. Dunkin, and E. E. Ferguson, *J. Chem. Phys.*, **58,** 3267 (1973).
(66) V. A. Bailey and J. M. Somerville, *Phil. Mag.* **17,** 1169 (1934).
(67) M. F. Skinker and J. V. White, *Phil. Mag.*, **46,** 630 (1923).
(68) M. W. Siegel, R. J. Cellota, J. L. Hall, J. Levine, and R. A. Bennett, *Phys. Rev. A*, **6,** 607 (1972).
(69) D. Spence and G. J. Schulz, *Phys. Rev. A*, **3,** 1968 (1971).
(70) H. F. Calcote and D. E. Jensen, *Adv. Chem. Ser.* **No. 58,** 291 (1966).
(71) L. M. Branscomb, *Phys. Rev.*, **148,** 11 (1966).
(72) H. Hotop, T. A. Patterson, and W. C. Lineberger, *Bull. Am. Phys. Soc.*, **18,** 810 (1973).
(73) F. K. Truby, *Phys. Rev.* **172,** 24 (1968).
(74) F. K. Truby, *Phys. Rev.*, **188,** 508 (1969).
(75) F. K. Truby, *Phys. Rev. A*, **4,** 613 (1971).
(76) L. C. Christophorou, R. N. Compton, and H. W. Dickson, *J. Chem. Phys.*, **48,** 1949 (1968).
(77) R. S. Davidow and D. A. Armstrong, *J. Chem. Phys.*, **48,** 1235 (1968).
(78) G. R. A. Johnson and J. L. Redpath, *Trans. Farad. Soc.*, **66,** 861 (1970).
(79) J. F. Paulson, *J. Chem. Phys.*, **52,** 963 (1970).
(80) A. V. Phelps, unpublished results as referenced in J. N. Bardsley, *J. Chem. Phys.*, **51,** 3384 (1969).
(81) E. E. Ferguson, F. C. Fehsenfeld, and A. L. Schemltekopf, *J. Chem. Phys.*, **47,** 3085 (1965).
(82) A. D. Walsh, *J. Chem. Soc.*, 2260 (1953); see also G. Herzberg, "Electronic Spectra of Polyatomic Molecules," Van Nostrand, Princeton, N.J., 1966.
(83) P. Gray and T. C. Waddington, *Proc. Roy. Soc., Ser. A*, **235,** 481 (1956).
(84) N. E. Bradbury and H. E. Tatel, *J. Chem. Phys.*, **2,** 835 (1934).
(85) S. Takeda and A. A. Dougal, *J. App. Phys.*, **31,** 412 (1960).
(86) R. E. Fox, P. R. Malmberg, and R. B. Gosser, *Rev. Sci. Instrum.*, **32,** 898 (1961).
(87) J. L. Pack, R. E. Voshall, and A. V. Phelps, *Phys. Rev.*, **127,** 2084 (1962).
(88) A. V. Phelps and R. E. Voshall, *J. Chem. Phys.*, **49,** 3246 (1968).
(89) J. M. Warman and R. W. Fessenden, *J. Chem. Phys.*, **49,** 4718 (1968).
(90) J. L. Moruzzi and J. T. Dakin, *J. Chem. Phys.*, **49,** 5000 (1968).
(91) E. L. Chaney and L. G. Christophorou, *J. Chem. Phys.*, **51,** 883 (1972).
(92) J. M. Warman, R. W. Fessenden, and G. Bakale, *J. Chem. Phys.*, **57,** 2702 (1972).
(93) D. Stelman, J. L. Moruzzi, and A. V. Phelps, *J. Chem. Phys.*, **56,** 4183 (1972).
(94) P. J. Chantry and A. V. Phelps, Westinghouse Research Labs., Annual Report, Contract DAH CO4-69-C-0094 ARPA 1842, 1970 (unpublished).
(95) B. H. Mahan and I. C. Walker, *J. Chem. Phys.*, **47,** 3780 (1967).
(96) V. A. J. Van Lint, J. Parez, M. E. Wyatt, and D. K. Nichols, Air Force Weapons Lab. Report RTD-TDR-63-3076, 1963 (unpublished).
(97) J. V. Hasted and S. Beg, *J. Brit. Appl. Phys.*, **16,** 1779 (1965).
(98) G. R. Freeman, *Chem. Phys. Lett.*, **8,** 241, 1971.
(99) L. Bouby, F. Fiquet-Fayard, and C. Bodere, *Int. J. Mass. Spectrom., Ion Phys.*, **7,** 415 (1971).
(100) L. G. Christophorou and R. P. Blaunstein, *Chem. Phys. Lett.*, **12,** 173 (1971).
(101) T. F. O'Malley, *Phys. Rev.*, **150,** 14 (1966).
(102) (a) J. N. Bardsley, A. Herzenberg, and F. Mandl, *Proc. Phys. Soc., London*, **89,** 305 (1966); (b) ibid., **89,** 321 (1966).
(103) T. F. O'Malley, *Phys. Rev.*, **155,** 59 (1967).
(104) T. F. O'Malley and H. S. Taylor, *Phys. Rev.*, **176,** 207 (1968).
(105) J. N. Bardsley, *J. Phys. B*, **1,** 349 (1968).
(106) C. J. Chapman and A. Herzenberg in ref 23, p 1164.
(107) F. Fiquet-Fayard, M. Sizun, and S. Goursaud, *J. Phys., (Paris)*, **33,** 669 (1972).
(108) D. T. Birtwistle and A. Modinos, *J. Phys. B*, **5,** 445 (1972).
(109) H. S. W. Massey, E. H. S. Burhop, and H. B. Gilbody, "Electronic and Ionic Impact Phenomena," Vol. II, Clarendon Press, Oxford, 1969.
(110) W. R. Henderson, W. L. Fite, and R. T. Brackmann, *Phys. Rev.*, **183,** 157 (1969); see also D. Spence and G. J. Schulz, ibid., **188,** 280 (1969).
(111) H. Feshbach, *Ann. Phys. (N.Y.)*, **5,** 357 (1958); **19,** 287 (1962).
(112) E. J. Shipsey, *J. Chem. Phys.*, **32,** 2274 (1970).
(113) W. B. Person, *J. Chem. Phys.*, **38,** 109 (1963).
(114) J. B. Blewett, *Phys. Rev.*, **49,** 900 (1936).
(115) J. E. Bailey, R. E. B. Makinson, and J. M. Somerville, *Phil. Mag.*, **24,** 177, 1937.
(116) S. A. A. Razzak and C. C. Goodyear, *J. Phys. D*, **2,** 1577 (1969).
(117) D. C. Frost and C. A. McDowell, *Can. J. Chem.*, **38,** 407 (1960).
(118) L. G. Christophorou and J. A. Stockdale, *J. Chem. Phys.*, **48,** 1956 (1968).
(119) M. E. Bradbury, *J. Chem. Phys.*, **2,** 827 (1934).
(120) V. A. Bailey and R. H. Healey, *Phil. Mag.*, **19,** 725 (1935).
(121) S. E. Bozin and C. C. Goodyear, *Brit. J. Appl. Phys.*, **18,** 49 (1967).
(122) R. Thorburn, *Proc. Phys. Soc., London*, **73,** 122 (1959).
(123) D. B. Dunkin, F. C. Fehsenfeld, and E. E. Ferguson, *Chem. Phys. Lett.*, **15,** 257 (1972).
(124) J. F. Burns, Carbide and Carbon Chemicals Co., K-25 Plant, Report K-1147, 1954 (unpublished).
(125) A. M. Mandl, *J. Chem. Phys.*, **59,** 3423 (1973).
(126) F. L. Mohler, *Phys. Rev.*, **26,** 614 (1925).
(127) T. R. Hogness and R. W. Harkness, *Phys. Rev.*, **32,** 784 (1928).
(128) R. H. Healey, *Phil. Mag.*, **26,** 940 (1938).
(129) R. Buchdahl, *J. Chem. Phys.*, **9,** 146 (1941).
(130) D. C. Frost and C. A. McDowell, *J. Chem. Phys.*, **29,** 964 (1958).
(131) M. A. Biondi, *Phys. Rev.*, **109,** 2005 (1958).
(132) R. E. Fox, *Phys. Rev.*, **109,** 2008 (1958).
(133) M. A. Biondi and R. E. Fox, *Phys. Rev.*, **109,** 2012 (1958).
(134) M. A. Biondi, private communication.
(135) C. C. Davis and T. A. King, "2nd International Conference on Gas Discharges," London, 11–15 Sept, 1972, IE, London, 1972, p 127.
(136) L. G. Christophorou, unpublished results.
(137) R. K. Curran and R. E. Fox, *J. Chem. Phys.*, **34,** 1590 (1961).
(138) G. J. Schulz, *J. Chem. Phys.*, **34,** 1778 (1961).
(139) P. J. Chantry, *J. Chem. Phys.*, **51,** 3369 (1969).
(140) J. N. Bardsley, *J. Chem. Phys.*, **51,** 3384 (1969).
(141) W. E. Wentworth, E. Chen, and R. Freeman, *J. Chem. Phys.*, **55,** 2075 (1971).
(142) J. H. Mullen, J. M. Madson, L. N. Medgyesi-Mitschang, T. C. Peng, and P. M. Doane, *Rev. Sci. Instrum.*, **41,** 1746 (1970).
(143) J. H. Mullen, J. M. Madson, and L. N. Medgyesi-Mitschang, *Proc. IEEE*, **59,** 605 (1971).
(144) J. H. Mullen, J. M. Madson, and L. N. Medgyesi-Mitschang, *AIAA J.*, **11,** 1031 (1973).
(145) F. C. Fehsenfeld, A. L. Schmeltekopf, H. I. Schiff, and E. E. Ferguson, *Planet. Space Sci.*, **15,** 373 (1967).
(146) F. C. Fehsenfeld and E. E. Ferguson, *Planet. Space Sci.*, **16,** 701 (1968).
(147) R. K. Curran, Westinghouse Research Labs Scientific Paper 908-3901-P4, Nov 1961 (unpublished).
(148) D. Spence and G. J. Schulz, *J. Chem. Phys.*, **58,** 1800 (1973).
(149) W. J. Miller and R. K. Gould, *Bull. Am. Phys. Soc.*, **19,** 149 (1974).
(150) J. Guillerez and L. Bouby, Laboratoire de Collisions Electroniques, Rapport Interne, C.E. No. 26, Orsay, 1972 (unpublished).
(151) J. Rademacher, L. G. Christophorou, and R. P. Blaunstein, *J. Chem. Soc., Faraday Trans. 2*, in press.
(152) G. D. Sides and T. O. Tiernan, Air Force Aerospace Research Laboratories, Report ARL TR 74-0105, 1974 (unpublished).
(153) N. A. Burdett and A. N. Hayhurst, *Nature, Phys. Sci.* **245,** 77 (1973).
(154) F. C. Fehsenfeld and C. J. Howard, *Bull. Am. Phys. Soc.*, **20,** 239 (1975).